

USE OF A MODIFIED SHIPS ALGORITHM FOR HURRICANE INTENSITY FORECASTS

T. N. Krishnamurti

**Department of Earth ,Ocean and Atmospheric Science
FLORIDA STATE UNIVERSITY**

67th IHC/Tropical Cyclone Research

Mar 7 2013



ABSTRACT

This work entails an improvement of the **SHIPS algorithm** by bringing into the predictors some dynamical parameters (derived from HWRF forecast of hurricanes) from the output in addition to the **statistical state variables** of SHIPS. We include all of the named storms of the 2012 hurricane season for the Atlantic basin. We have explored various post processing methods to examine the impacts of the post processed dynamical variables. In this context we have included the intensity forecasts from **SPICE (SPC3)**. The **dynamical variables** are shown to add to the skills of SHIPS and SPICE (SPC3).

SHIPS

- 21 total predictors used
- Atmospheric Predictors from GFS
- SST from Reynolds weekly fields
- Predictors from satellite data
 - Ocean Heat content from altimetry
 - GOES IR window channel brightness temperature

SHIPS Predictors

- Persistence
 - 12hr intensity change
 - Max winds at $t = 0$ (V_{max})
 - $V_{max} * 12$ hr intensity change
- Upper Level Temperature
 - 200mb Temperature
 - 250mb Temperature (relative to threshold temperature of -44°C)
- Sea Surface Potential
 - Difference between forecasted Max Potential Intensity and $t = 0$ intensity
 - Sea Surface Potential squared
- GFS Vortex Tendency
 - Change in GFS 0-600km average symmetric tangential wind at 850mb

SHIPS Predictors cont...

- Zonal Storm motion (SPDX)
 - X component of motion from lat-lon position (finite differencing of forecast position from NHC)
- Steering Layer Pressure
 - Layer where wind best resembles storm motion
- Satellite Predictors
 - Standard Deviation of GOES Brightness Temperature (0-200km) *
Vmax
 - Percent area where GOES $T_b < -20^{\circ}\text{C}$ (50-200km)
 - Ocean Heat Content
- Theta-E Excess
 - Theta-E difference (positive only) between a parcel lifted from the surface and its environment (200-800km average)

SHIPS Predictors cont...

- 850-200mb Shear
 - Magnitude of shear with vortex removed averaged from 0-500km (SHR)
 - Heading of above predictor
 - SHR * Latitude
 - SHR * Vmax
- 200mb Divergence
 - Averaged from 0-1000km
- 850mb Vorticity
 - Averaged from 0-1000km
- Mid Level Relative Humidity
 - Averaged from 700-500mb

SHIPS Forecast Methodology

- Multiple linear regression applied to normalized independent and dependant variables

$$\frac{(value - mean)}{stddev}$$

- Final forecast takes form of:

$$\left(A * \sum \frac{value(p) - mean(p)}{stddev(p)} \right) + B$$

where A is the standard deviation of the change in intensity, B is the mean change in intensity of all cases, and p represents the predictors.

THIS ENTIRE STUDY UTILIZES REGRESSIONS FOR INTENSITY TENDENCIES.

SPICE (Statistical Prediction of Intensity from a Consensus Ensemble) has been developed as a combination of the official **SHIPS** and **LGEM (logistic growth equation model)** intensity guidance, as well as SHIPS and LGEM runs based on the large-scale environments in the GFDL and HWRF regional models. The six total forecasts are combined into two unweighted consensus: one from the three SHIPS forecasts and one from the three LGEM forecasts. The two unweighted consensus are then combined into one weighted consensus, with the weights determined empirically from the **2010-2011 official SHIPS and LGEM** sample. These weights favored the SHIPS consensus in the early time periods, shifting to the LGEM consensus being weighted more heavily after about 36 hours. Retrospective tests of SPICE over the 2010-2011 Atlantic hurricane seasons indicated that **SPICE outperformed both SHIPS and LGEM** at all lead times, and the improvements were statistically significant at almost all times.

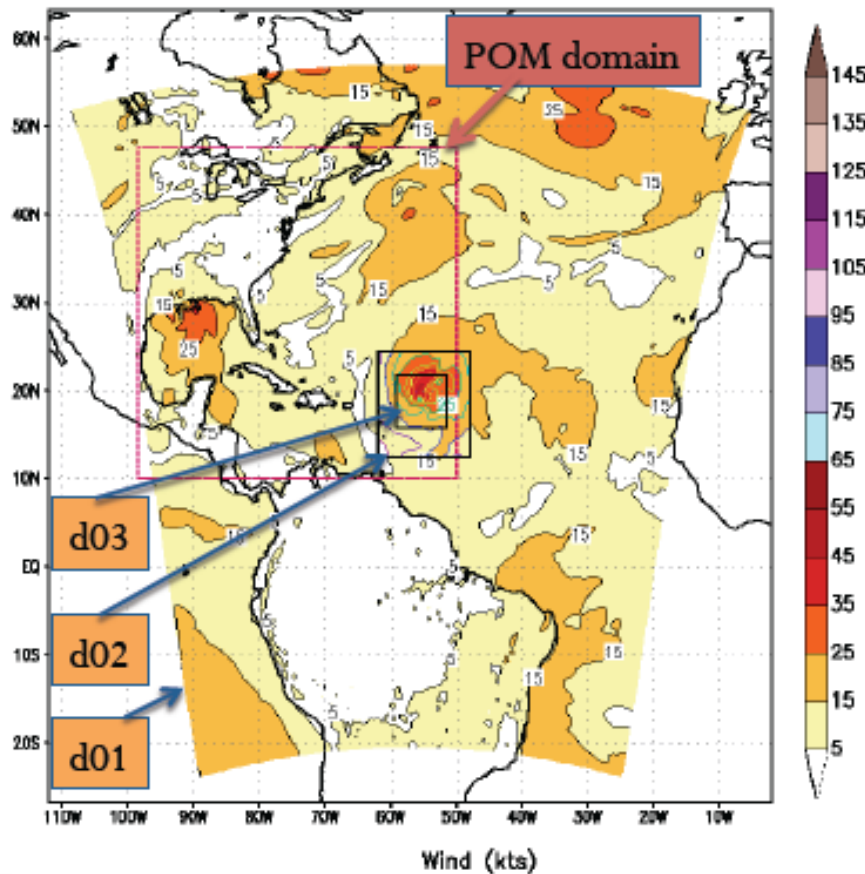
DATA SETS USED FOR FSU DIAGNOSTICS:

The data sets we used for the extended SHIPS were based on a reanalysis that was provided to us by the HWRF group. It carried the following steps:

1. Start with GFS analysis at T382L64 , transform grid separation to roughly 35 km
2. Remove vortex from GFS using GFDL method, Kurihara et al
3. Use HWRF's 12 hour forecast as a first guess to redefine a new initial vortex
4. Use above within GFS to re-assimilate that vortex along with the dropwindsonde data sets.

HWRF 2012 grid configuration

Initialized at 2011090300 – 12 (h) fcst valid at 2011090312
HWRF Domain Kafia 12L



Atmospheric configuration

- Horizontal grid spacing: 27, 9, 3 km
- Inner nests move to follow storm
- Domain location vary from run to run depending on storm location
- 42 vertical levels
- Model top 50 hPa

Oceanic configuration

- Horizontal grid spacing: 18 km
- Size, location of grid depends of location of storm
- Pacific
 - 1-D (column) model
 - 16 vertical levels
- Atlantic
 - 3-D model
 - 23 vertical levels

Towards High-Resolution HWRF implementation in FY2012: A major step towards improving intensity forecast skill and address rapid intensity.

Three atmospheric telescoping nested domains:

- **27km outer domain 75x75 degree**
- **9km intermediate nest ~11x10 degree**
- **3km inner-most nest ~6x5 degree**

The **diagnostic parameters** are computed from HWRF Forecast for many hurricane cases during the **2010 and 2011** seasons. We have used inner nest (3km resolution) data for computation of FSU Diagnostic parameters.

Vertical differential of heating (for the complete PV equation), **shear to curvature kinematics** and the **transformation of divergent kinetic energy into rotational kinetic energy** are all evaluated from the final HWRF analysis at the 850hPa level. The **advection of earths and relative angular momentum** are averaged over a three dimensional box that covers the same horizontal area as above, in the vertical the box average extends from the surface to 100 hPa.

- These computations are carried out every 12 hours and are designed to provide guidance for 12 hourly intensity forecasts.

List of FSU Diagnostic Parameters

1. **Vertical Differential of Heating**
2. **Transformation of Shear to Curvature Vorticity**
3. **Energy Exchange from the Divergent to the Rotational Kinetic Energy in the Inner Core**
4. **Angular Momentum**

Shear to curvature

5. Transformation of shear to curvature vorticity:

The transformation of shear vorticity to curvature vorticity is one of the parameters that is important for the rapid intensification of a hurricane. The curvature vorticity and the shear vorticity in natural co-ordinates can be written following Bell and Keyser (1993) and Viudez and Haney (1996) as:

$$\frac{d}{dt} \left(f + V \frac{\partial \alpha}{\partial s} \right) = - \frac{\partial V}{\partial s} \frac{d\alpha}{dt} - \frac{\partial}{\partial n} \left(\frac{\partial \Phi}{\partial s} \right) - \left(f + V \frac{\partial \alpha}{\partial s} \right) \nabla_{\mathbf{p}} \cdot \mathbf{V} - V \frac{\partial \omega}{\partial s} \frac{\partial \alpha}{\partial p} \quad (10)$$

$$\frac{d}{dt} \left(- \frac{\partial V}{\partial n} \right) = \frac{\partial V}{\partial s} \frac{d\alpha}{dt} + \frac{\partial}{\partial n} \left(\frac{\partial \Phi}{\partial s} \right) - \left(- \frac{\partial V}{\partial n} \right) \nabla_{\mathbf{p}} \cdot \mathbf{V} + \frac{\partial \omega}{\partial n} \frac{\partial V}{\partial p} \quad (11)$$

and the tendency equation for absolute vorticity can be written as:

$$\frac{d}{dt} \left(f + V \frac{\partial \alpha}{\partial s} - \frac{\partial V}{\partial n} \right) = - \left(f + V \frac{\partial \alpha}{\partial s} - \frac{\partial V}{\partial n} \right) \nabla_{\mathbf{p}} \cdot \mathbf{V} - V \frac{\partial \omega}{\partial s} \frac{\partial \alpha}{\partial p} + \frac{\partial \omega}{\partial n} \frac{\partial V}{\partial p} \quad (12)$$

Here V and ϕ denote the scalar wind and geopotential respectively and α is the angle subtended by the velocity vector with respect to the x-axis (positive in the anticlockwise orientation). The first and second terms of equation on the right-hand side (10) and (11) describes the conversion between shear and curvature vorticity. A computational form for the shear to curvature conversion term in the Cartesian co-ordinates is also given by Bell and Keyser (1993) as:

$$\frac{\partial V}{\partial s} = \frac{1}{V^2} [(u^2 u_x + v^2 v_y) + uv(v_x + u_y)] \quad (13)$$

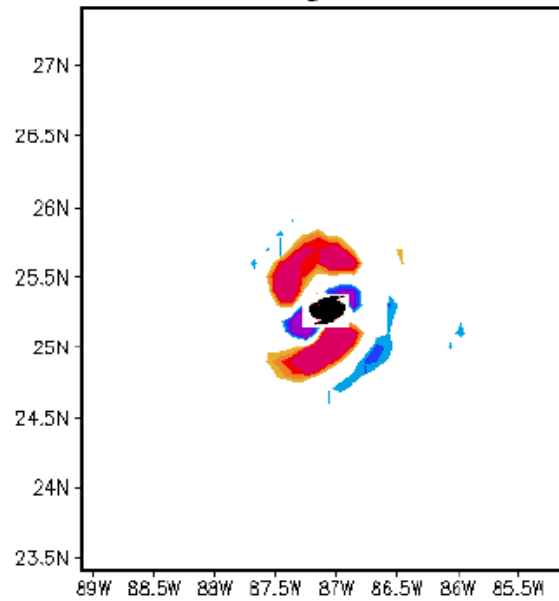
$$\frac{d\alpha}{dt} = \frac{1}{V^2} (v\phi_x - u\phi_y) \quad (14)$$

$$\begin{aligned} \frac{\partial}{\partial n} \left(\frac{\partial \phi}{\partial s} \right) &= \frac{1}{V^2} [(u^2 - v^2)\phi_{xy} - uv(\phi_{xx} - \phi_{yy})] \\ &+ \frac{uv}{V^4} [(v_x + u_y)(v\phi_x - u\phi_y) + vu_x\phi_y - uv_y\phi_x] \end{aligned}$$

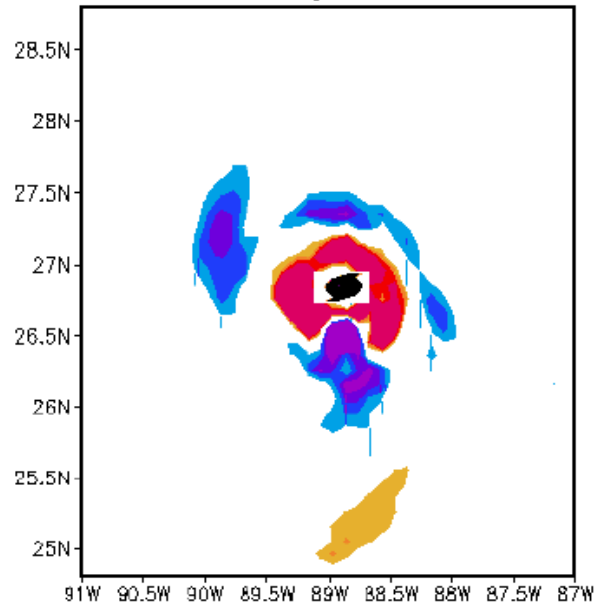
$$\frac{1}{4} (u^3 v_y \phi_y - v^3 u_x \phi_x) \quad (15)$$

The equation describing this transfer carries both dynamical and thermodynamical forcing. Hence we cannot entirely attribute this seemingly kinematic exchange to just barotropic processes. The presence of divergence and vertical velocity in some of the terms in the right hand side, implicitly, are forced by the baroclinic and heating terms of a complete system of equations from where these are derived. Within a hurricane's inner core all of the effects are present and hence the transformation of shear vorticity to curvature vorticity can be due to barotropic plus all of these interactive processes.

28 August 00z

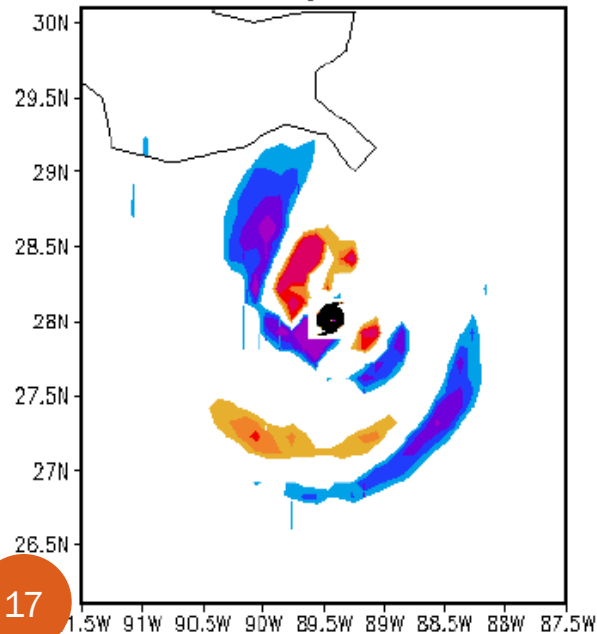


28 August 12z

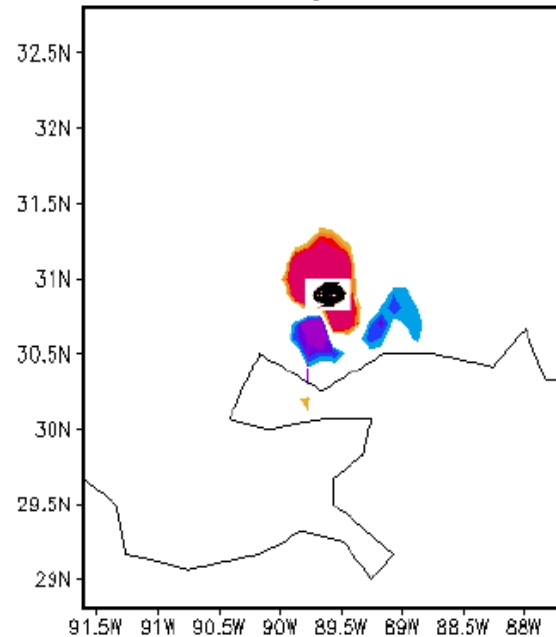


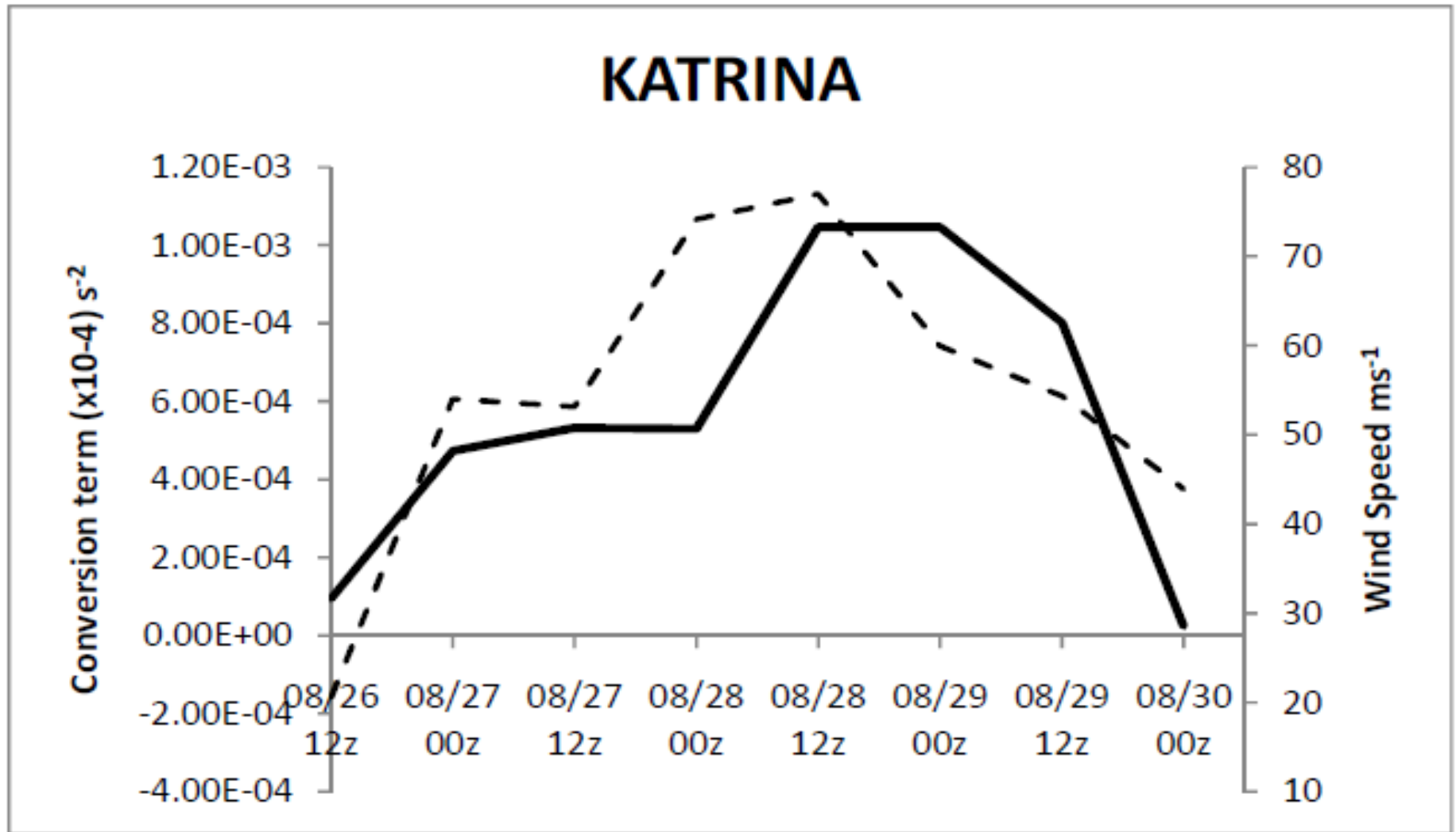
Spatial map of the conversion form shear to curvature vorticity at 850 hPa for hurricane Katrina. The units are $(\times 10^{-4} s^{-2})$.

29 August 00z

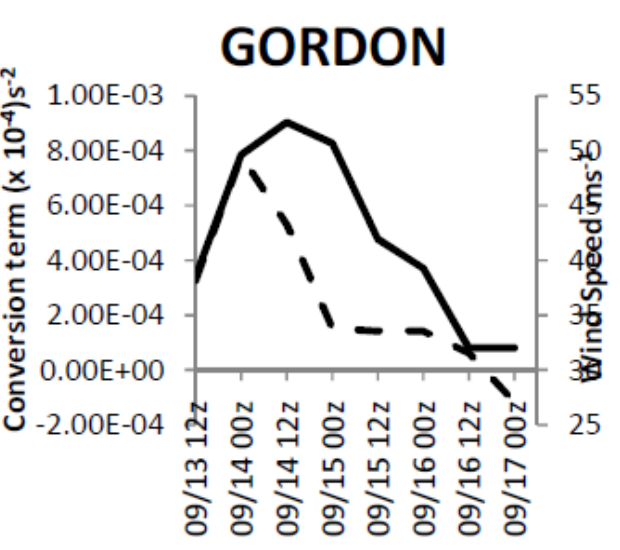
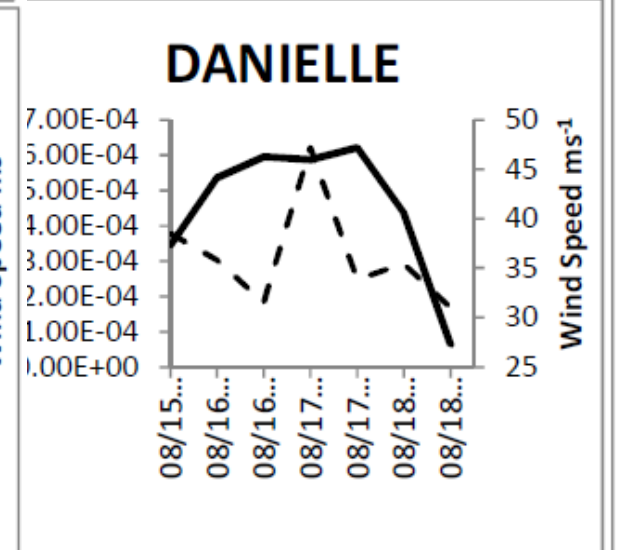
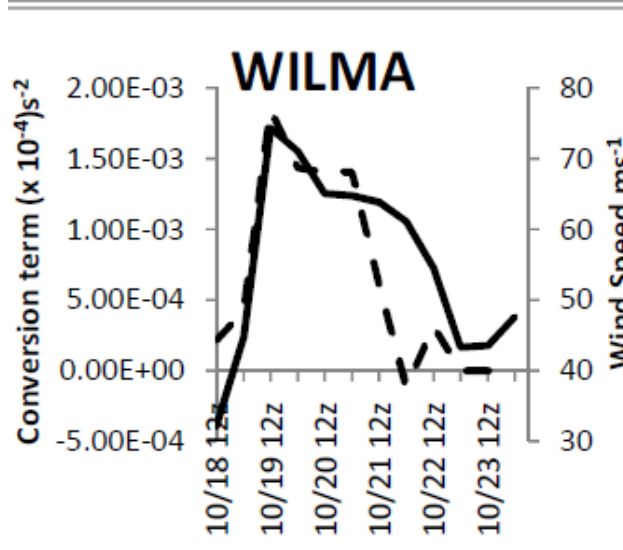
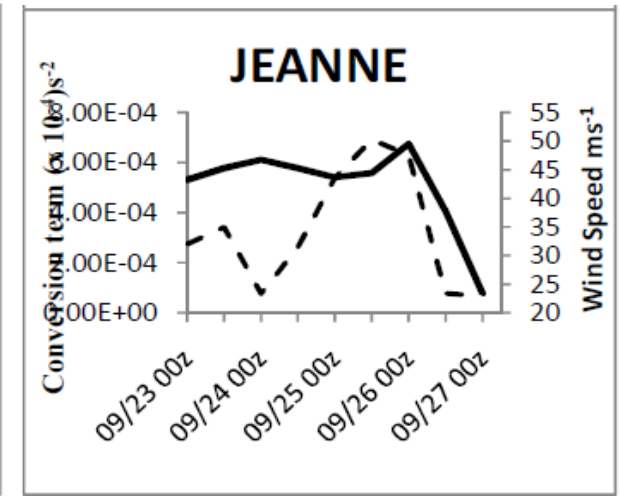
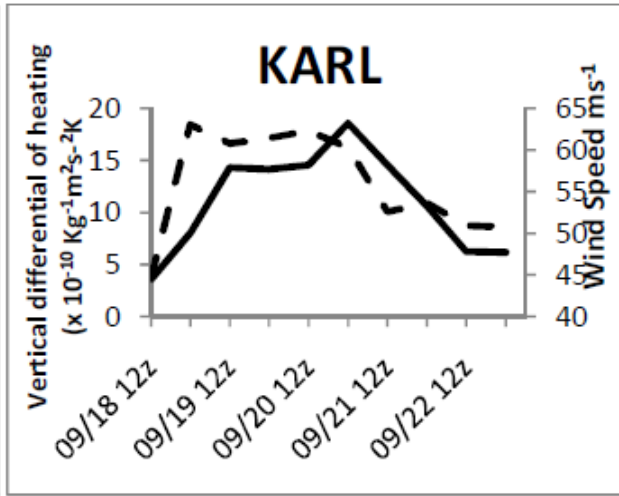
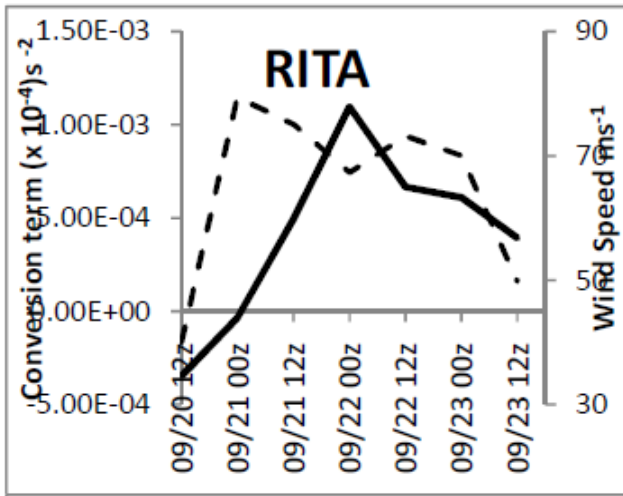


29 August 12z





Time history of the shear to curvature conversion term, at 850hPa (dashed line) and the intensity of Hurricane Katrina.



Time histories shear to curvature conversion term, at 850hPa (dashed line) and the intensity of the storm for the various storms taken from the HWRF analysis.

Diabatic Potential Vorticity over the Global Tropics

10.1 Diabatic Potential Vorticity Equation

The diabatic potential vorticity equation takes into account the heat sources and sinks, and thus provides a more accurate formulation of the problem. The natural framework for the diabatic potential vorticity equation uses the potential temperature as a vertical coordinate. The quasi-static version of the complete Ertel Potential Vorticity Equation in such isentropic coordinates is expressed by (Bluestein, 1993) as:

$$\frac{d}{dt} \left(-\zeta_{a\theta} g \frac{\partial \theta}{\partial p} \right) = \left(-\zeta_{a\theta} g \frac{\partial \theta}{\partial p} \right) \frac{\partial}{\partial \theta} \frac{d\theta}{dt} + \left\{ \nabla \frac{d\theta}{dt} \cdot \frac{\partial (\mathbf{V} \times \mathbf{k})}{\partial \theta} \right\} g \frac{\partial \theta}{\partial p} - \{ \nabla \cdot (\mathbf{F} \times \mathbf{k}) \} g \frac{\partial \theta}{\partial p} \quad (10.4)$$

where the isentropic absolute vorticity is given by:

$$\zeta_{a\theta} = \left(\frac{\partial v}{\partial x} \right)_{\theta} - \left(\frac{\partial u}{\partial y} \right)_{\theta} + \frac{u}{a} \tan \varphi + f \quad (10.5)$$

and the isentropic potential vorticity is expressed by:

$$\zeta_{p\theta} = -g\zeta_{a\theta} \frac{\partial\theta}{\partial p} \quad (10.6)$$

where φ and θ are the latitude and potential temperature respectively. The reference to quasi-static indicates that vertical motion and its acceleration appears in equation 10.4 and yet the system is not non-hydrostatic i.e., vertical acceleration does not change gravity. The dry static stability, $-g\frac{\partial\theta}{\partial p}$, is generally positive unless super-adiabatic layers are present. The absolute and the potential vorticities, $\zeta_{a\theta}$ and $\zeta_{p\theta}$, are generally positive over the Northern Hemisphere and are generally negative over the Southern Hemisphere, except for the cross-equatorial meanders of the zero potential vorticity isopleth.

By substituting equation (10.6) into equation (10.4) we find that the local rate of change of isentropic potential vorticity is given by:

$$\frac{\partial}{\partial t} \zeta_{p\theta} = -\mathbf{V} \cdot \nabla \zeta_{p\theta} - \frac{d\theta}{dt} \frac{\partial \zeta_{p\theta}}{\partial \theta} + \zeta_{p\theta} \frac{\partial}{\partial \theta} \frac{d\theta}{dt} + \left\{ \nabla \frac{d\theta}{dt} \cdot \frac{\partial (\mathbf{V} \times \mathbf{k})}{\partial \theta} \right\} g \frac{\partial \theta}{\partial p} - \left\{ \nabla \cdot (\mathbf{F} \times \mathbf{k}) \right\} g \frac{\partial \theta}{\partial p} \quad (10.7)$$

In other words, on an isentropic surface,

<i>Local rate of</i>		<i>Horizontal</i>		<i>Vertical</i>		<i>Vertical</i>		<i>Horizontal</i>		<i>Friction</i>
<i>change</i>	=	<i>advection of</i>	+	<i>advection of</i>	+	<i>differential of</i>	+	<i>differential of</i>	+	<i>term.</i>
<i>of PV</i>		<i>PV</i>		<i>PV</i>		<i>heating</i>		<i>heating</i>		

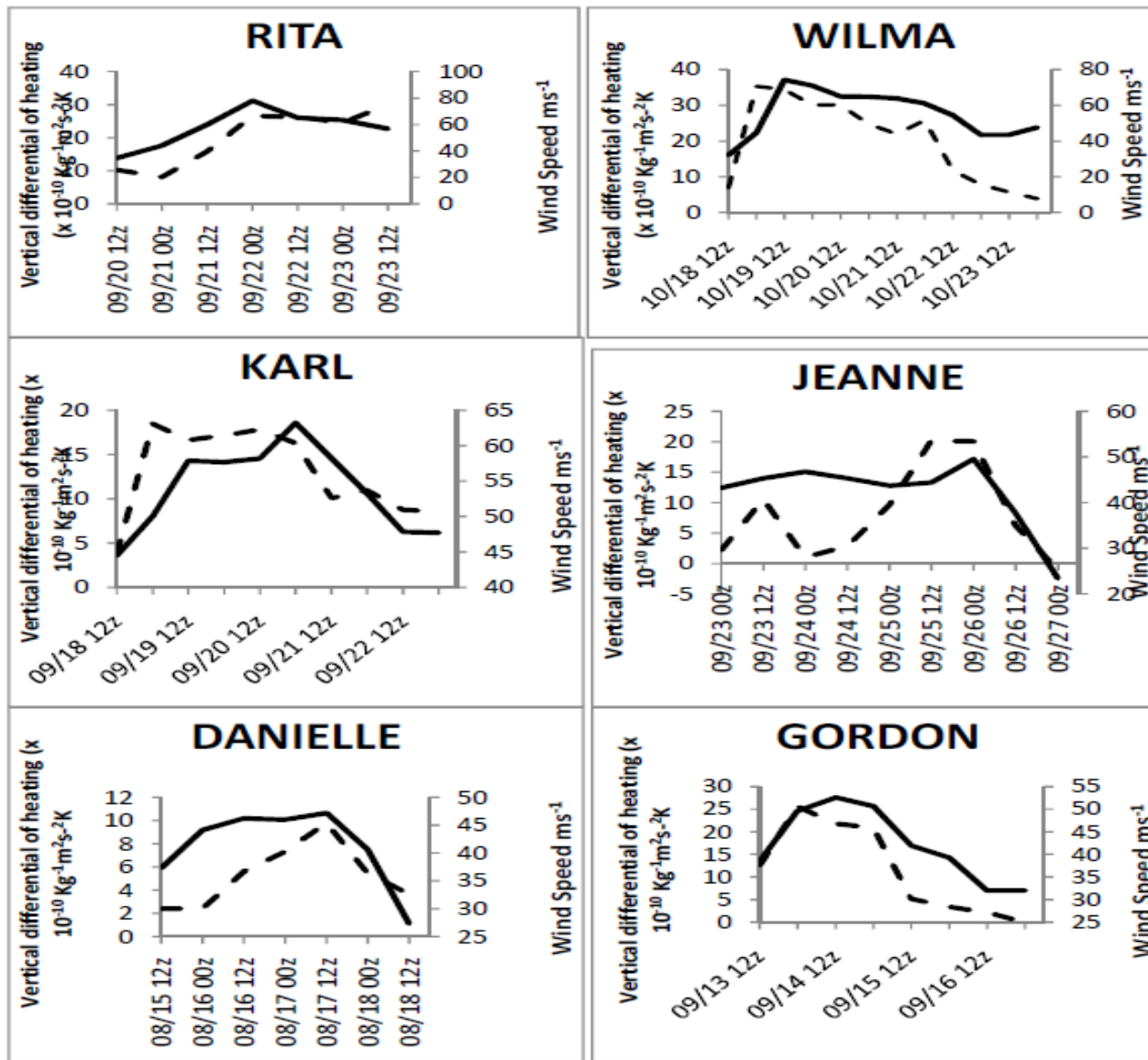
If the last three terms on the right hand side are neglected, equation 10.7 reduces to the familiar adiabatic equation for the conservation of potential vorticity. Retaining these three terms allows us to account for the generation or destruction of potential vorticity due to horizontal or vertical heating differentials and friction. Calculation of the potential vorticity budget involves the calculation of all terms using variables interpolated to isentropic surfaces.

Application of the Diabatic Potential Vorticity Equation to Hurricanes

The hurricanes are characterized by substantial amounts of deep cumulus convection. This deep convection is particularly strong along the eye wall and the rain bands. There, one of the most important diabatic contributions to the potential vorticity is given by the vertical differential heating term, *i.e.*, $\zeta_{p\theta} \frac{\partial}{\partial \theta} \frac{d\theta}{dt}$. For the Northern Hemisphere, hurricane regions generally have positive potential vorticity $\zeta_{p\theta}$. Below the level of maximum convection, $\frac{\partial}{\partial \theta} \frac{d\theta}{dt}$ is positive. This, combined with the positive potential vorticity, leads to $\frac{\partial}{\partial t} \zeta_{p\theta} > 0$. In regions of heavy precipitation, such as that found in the eye wall of a hurricane, the difference in the heating rate $\frac{d\theta}{dt}$ can reach up to about 50 K day^{-1} over an atmospheric depth of 5 km . Over this depth of atmosphere, the potential temperature changes by about 5 K . All this translates to $\frac{\partial}{\partial \theta} \frac{d\theta}{dt} \approx 10^{-4} \text{ s}^{-1}$.

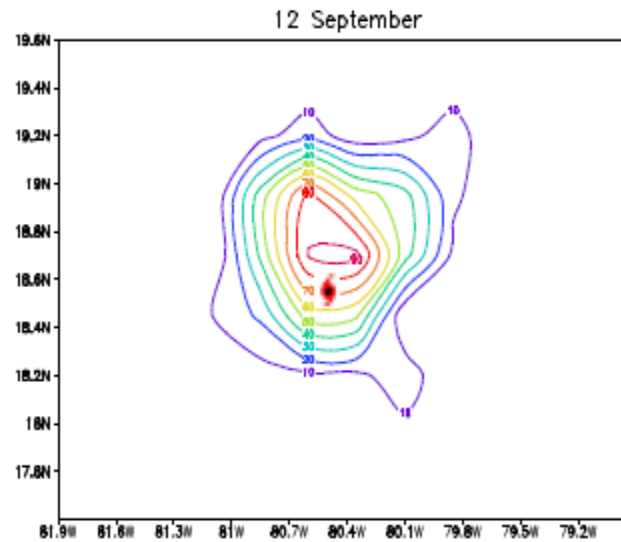
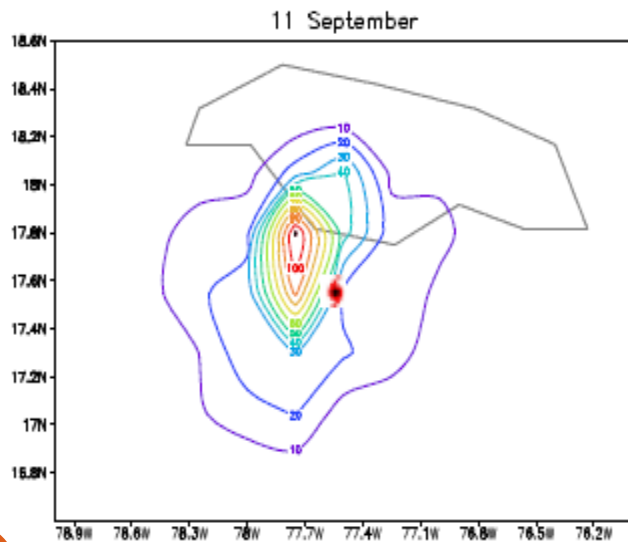
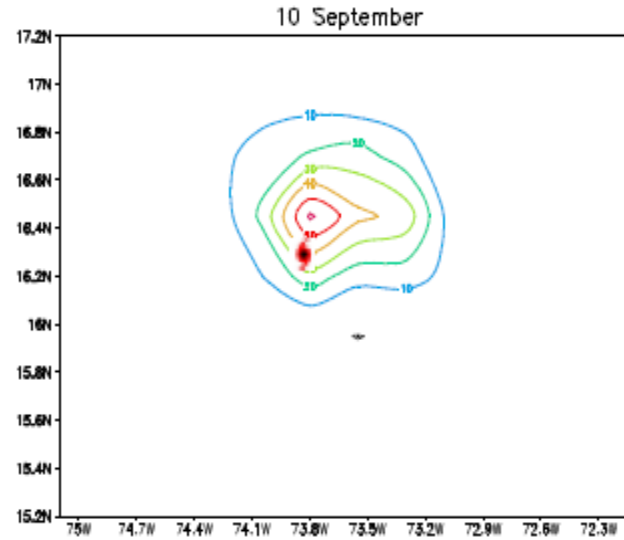
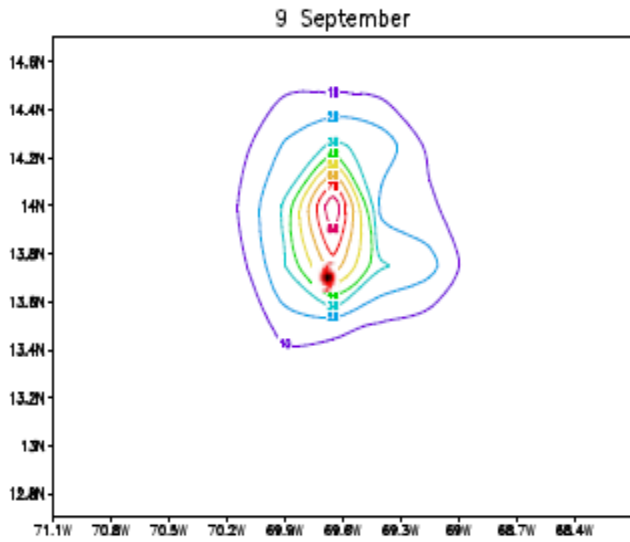
The potential vorticity of a hurricane is on the order of $10^{-6} \text{ kg}^{-1} \text{ m}^2 \text{ s}^{-1} \text{ K}$. Thus the rate of change of potential vorticity resulting from such differential heating can be quite large, of the order of $10^{-10} \text{ kg}^{-1} \text{ m}^2 \text{ s}^{-2} \text{ K}$, which is comparable to (or even somewhat larger than) the horizontal advection of potential vorticity in a hurricane. These two effects – differential heating and horizontal advection of potential vorticity – can contribute to an increase of intensity of the hurricane from the following arguments. Both the horizontal advection of potential vorticity and the diabatic potential

vorticity contribution from $\zeta_{p\theta} \frac{\partial}{\partial \theta} \frac{d\theta}{dt}$ can lead to a local increase of potential vorticity. In regions of heavy rains, convergence in the lower troposphere reduces the dry static stability (see eq. 10.2). Since the potential vorticity is increasing while the dry static stability is decreasing, an increase of absolute vorticity must take place. Since the Coriolis parameter is virtually constant for slow zonally moving disturbances, this results in a large increase of relative vorticity, which implies a stronger cyclonic circulation, *i.e.*, a stronger storm.



Time histories of vertical differential of heating at 850 hPa ($\times 10^{-10} \text{ Kg}^{-1} \text{ m}^2 \text{ s}^{-2} \text{ K}$, dashed line) and intensity of the storm for the various storms taken from the HWRf analysis.

Vertical Differential of Heating



Contour plots of vertical differential of heating at 850 hPa ($\times 10^{-10} \text{ Kg}^{-1}\text{m}^2\text{s}^{-2}\text{K}$) for hurricane IVAN 9 September through 12 September 2004 at 00z. The storm center is also marked.

Psi –Chi interaction

$$V_H = V_\psi + V_\chi \quad (6)$$

where $V_\psi = K \times \nabla\psi$ and $V_\chi = -\nabla\chi$. Here ψ is the streamfunction and χ is the velocity potential. The energy equations in terms of these components can be expressed by the relation given by Krishnamurti et al., 1982 as :

$$\begin{aligned} \frac{\partial}{\partial t} K_\psi = & \nabla \cdot \psi \nabla \frac{\partial \psi}{\partial t} - \psi \nabla \cdot f \nabla \chi - \psi \nabla \chi \cdot \nabla (\nabla^2 \psi) - \psi \nabla^2 \chi \nabla^2 \psi + \psi \omega \frac{\partial}{\partial p} \nabla^2 \psi + \psi \nabla \omega \nabla \frac{\partial \psi}{\partial p} \\ & - \psi J \left(\omega, \frac{\partial \chi}{\partial p} \right) + \psi J(\psi, \nabla^2 + f) + F_\psi \end{aligned} \quad (7)$$

$$\begin{aligned} \frac{\partial}{\partial t} K_\chi = & \nabla \cdot \chi \nabla \frac{\partial \chi}{\partial t} - \chi \nabla^2 \phi + \chi \nabla \cdot f \nabla \psi + \chi (\nabla^2 \psi)^2 - \frac{\chi \nabla^2 (\nabla \psi^2)}{2} - \frac{\chi \nabla^2 (\nabla \chi^2)}{2} + \chi \nabla \psi \cdot \nabla (\nabla^2 \psi) - \\ & - \psi J \left(\omega, \frac{\partial \chi}{\partial p} \right) + \psi J(\psi, \nabla^2 + f) + F_\chi \end{aligned} \quad (8)$$

The energy equation for the rotational component can then be then be written as :

$$\frac{\partial}{\partial t} \overline{K_\psi} = \overline{f \nabla \psi \cdot \nabla \chi} + \overline{\nabla^2 \psi \nabla \psi \cdot \nabla \chi} + \overline{\nabla^2 \chi (\nabla \psi^2) / 2} + \overline{\omega J \left(\psi, \frac{\partial \chi}{\partial p} \right)} + B_\psi + \overline{F_\psi} \quad (9)$$

Here B_ψ is the boundary flux.

The terms on the right side of equations (9) with double overbars denote the ψ, χ interactions.

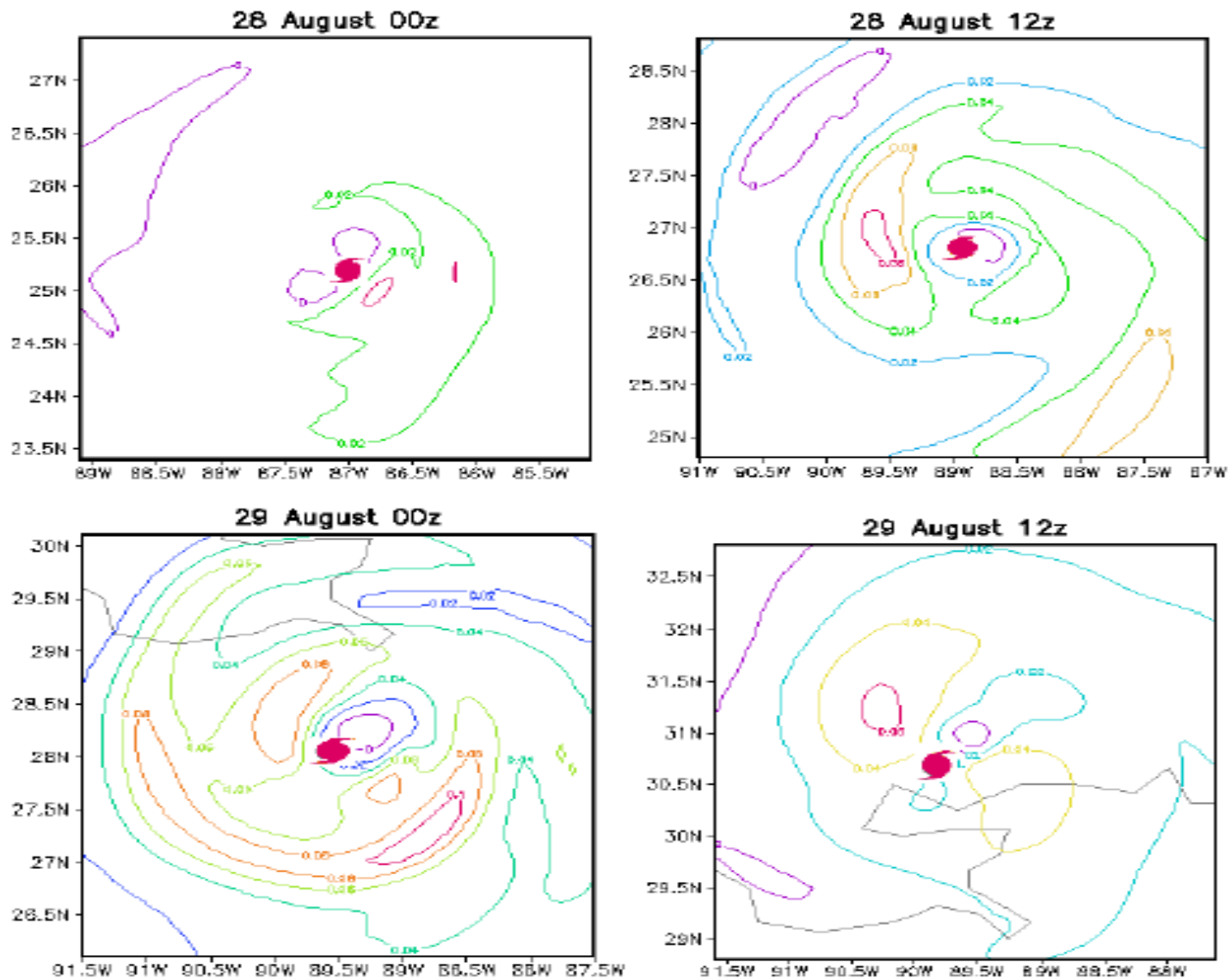


Figure 4a: Spatial distribution of the term $fV\psi V\chi$ (at 850hPa) for hurricane Katrina. The position of the storm center is marked. The contours are drawn with an interval of 0.02. Units $m^2 s^{-3}$.

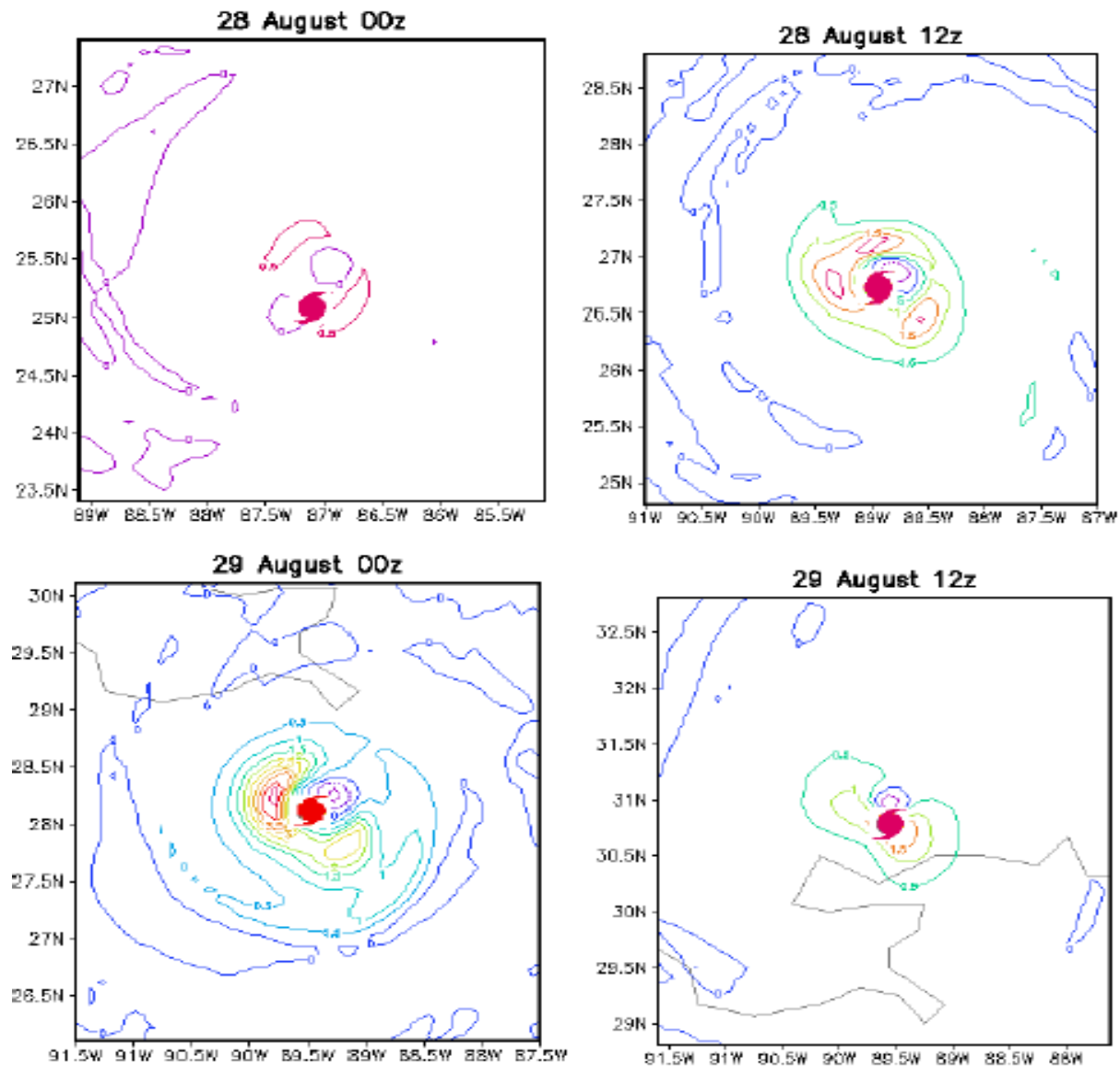
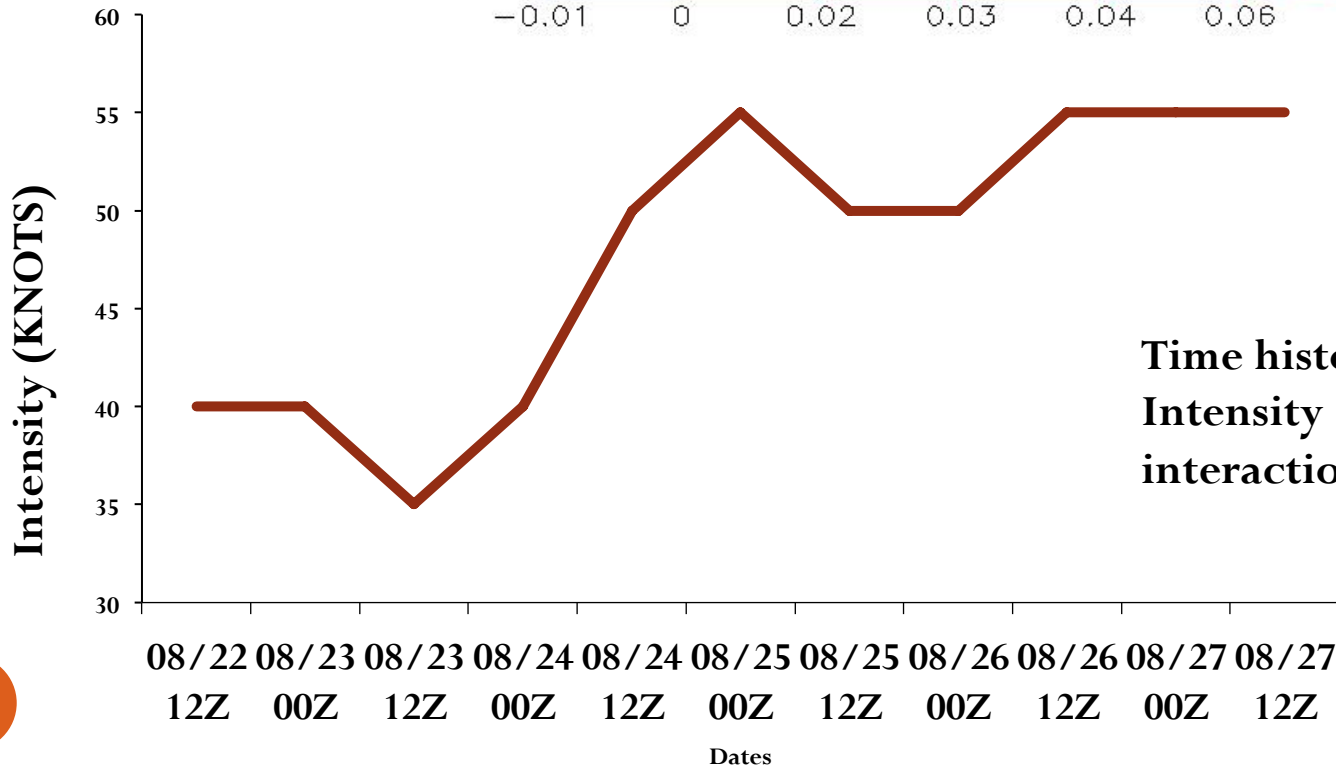
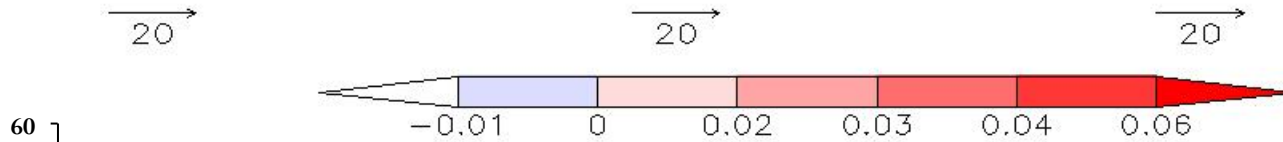
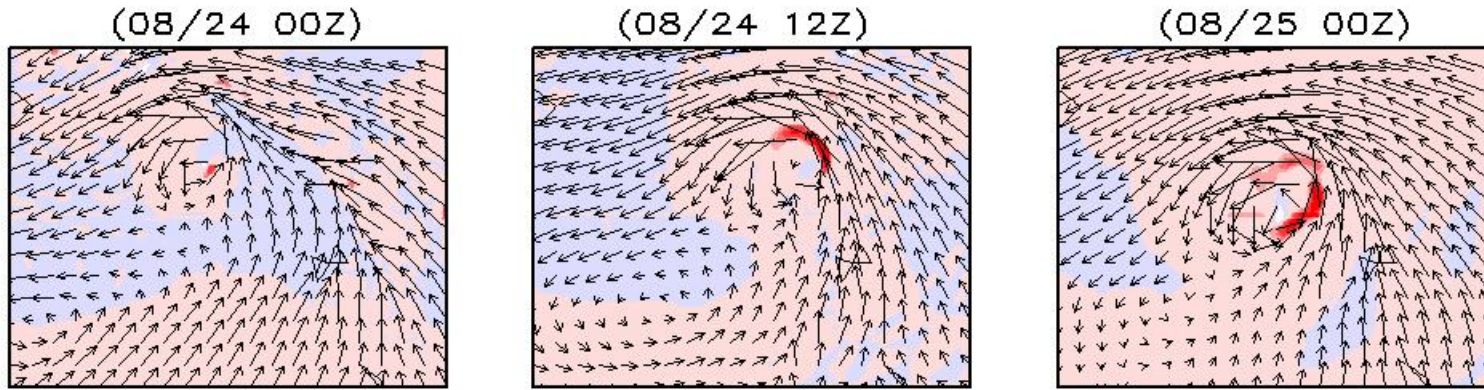


Figure 4b: Spatial distribution of the term $\nabla^2 \psi \nabla \psi \cdot \nabla \chi$ (at 850 hPa) for hurricane Katrina. The position of the storm center is marked. The contours are drawn with an interval of 0.5. Units $\text{m}^2 \text{s}^{-3}$.

Total Psi-Chi interaction for ISAAC 2012



Time history of Observed Intensity (Kt) and total Psi-Chi interaction terms

Angular Momentum

3.1 The Advection of Relative Angular Momentum

Angular momentum has long been used as a diagnostic variable for tropical cyclone analysis. Eliassen (1951) and Palmen and Riehl (1957) were among the first to use angular momentum as a tool for the diagnosis of tropical cyclone structure and intensification processes. More recently, Krishnamurti et al. (2005) and (2007) examined the role of angular momentum transport in tropical cyclone intensity change. Krishnamurti et al. (2005) proposed that parcels of air at large radii from the center of a tropical cyclone are brought into the storm's interior along inflow channels. When the parcel reaches at the inner core of the storm, the maximum surface winds are determined by the value of the angular momentum with which the parcel arrives. Martin (2009) examined the relationship between the horizontal advection of angular momentum and storm strength, and proposed that angular momentum could be used as a predictor in a statistical setting such as SHIPS.

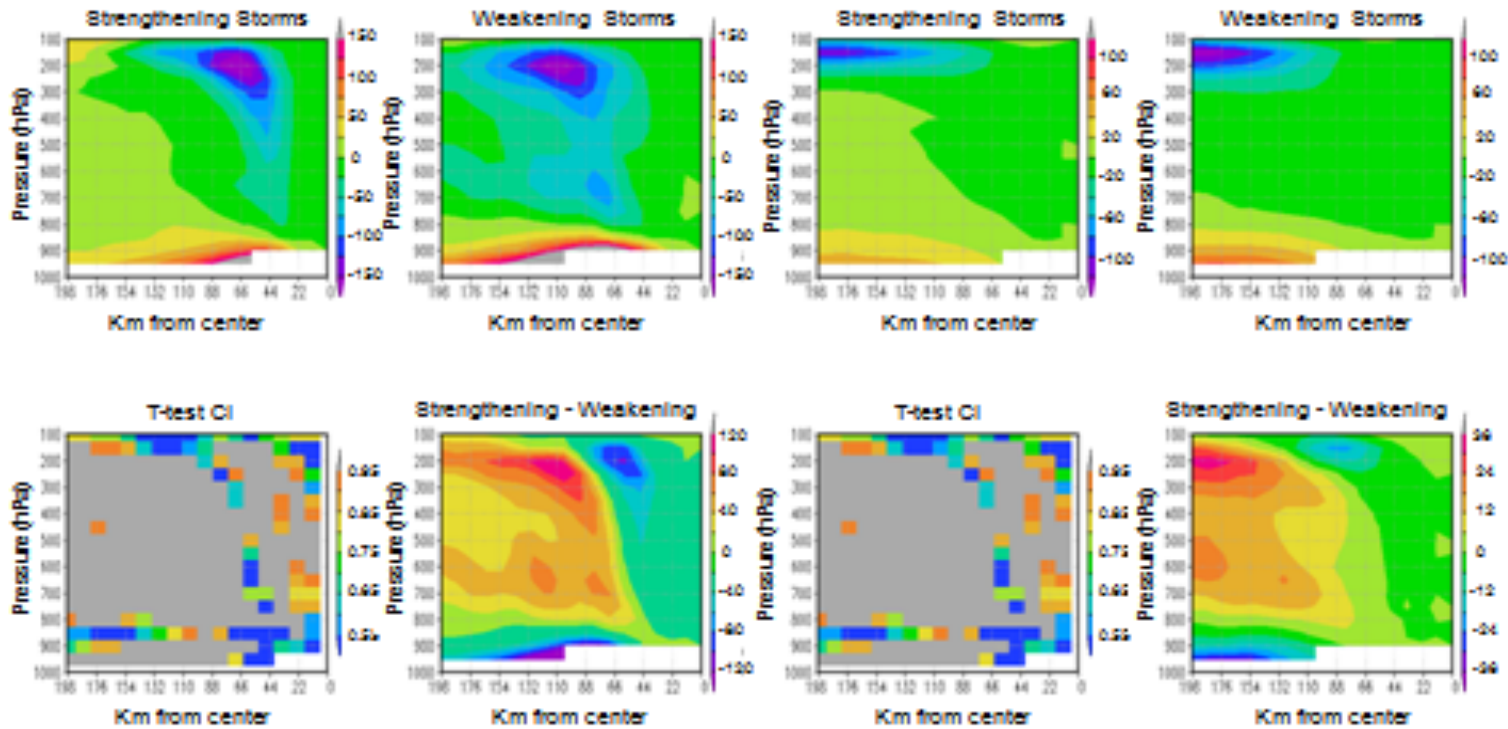
Martin (2009) defined the equation for absolute angular momentum per unit mass of air in storm relative cylindrical coordinates as

$$M = u_{\theta}r + f_0 \frac{r^2}{2}, \quad (3.1)$$

where u_{θ} is the wind speeding the azimuthal (θ) direction, f_0 is the Coriolis parameter (considered constant), and r is the radial distance from the storm center. This may be broken up into two contributions. The first is the angular momentum that arises due to the rotation of air about the center of the tropical cyclone, while the second is the contribution due to the rotation of the Earth. Simon et al. (2010) examined the advection of both terms and found that the horizontal advectons of relative angular momentum had the best relationship with tropical cyclone intensity changes. The advection is expressed as

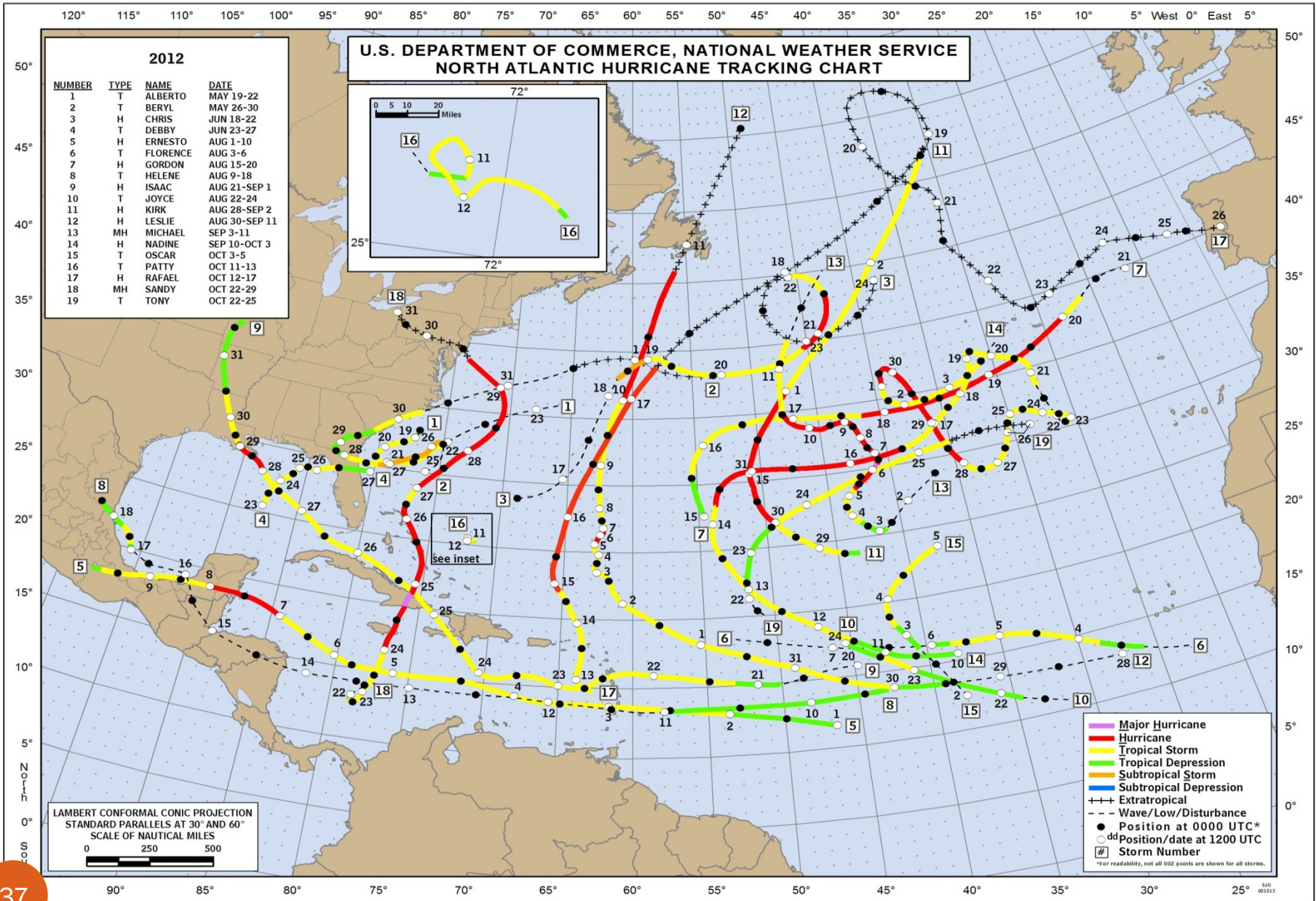
$$AR = -u \cdot \nabla M_R, \quad (3.2)$$

where AR is the advection of relative angular momentum, u is the two dimensional wind velocity vector, and M_R is the relative angular momentum. Figure 3.1 shows the results of a statistical t test comparing composites of strengthening and weakening category 2 or stronger hurricanes. Areas shaded in grey where the composites are significantly different at the 95% level.



Cross-section composites of horizontal advection in storms category 2 and higher for (a) Earth's angular momentum and (b) Relative angular momentum

ALL THE NAMED STORMS OF 2012

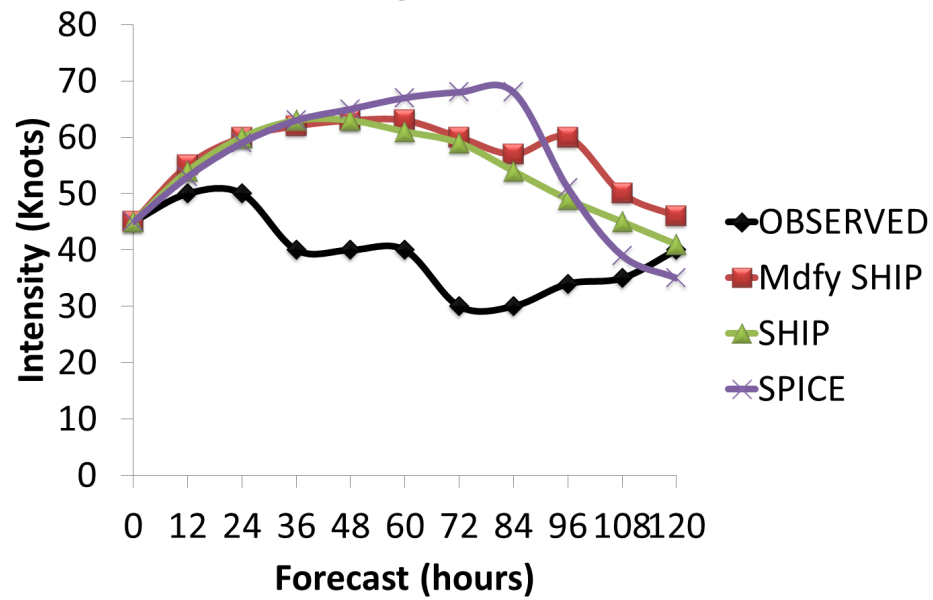


2012 Atlantic Basin Tropical Cyclones

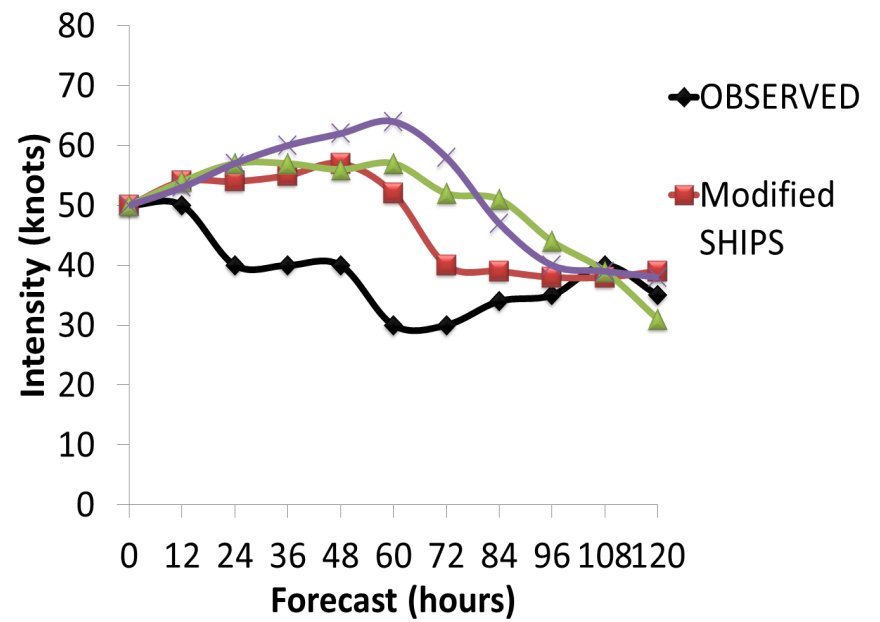
Type/ Cat	Name	Dates	Max Wind (mph)	Min Press (mb)	Deaths	U.S. Damage
TS	Alberto	19 – 22 May	60	995		
TS	Beryl	26 – 30 May	70	992	1	
H1	Chris	18 – 22 June	85	974		
TS	Debby	23 – 27 June	65	990	5	\$250M
H2	Ernesto	1 – 10 Aug	100	973	7	
TS	Florence	3 – 6 Aug	60	1002		
H2	Gordon	15 – 20 Aug	110	965		
TS	Helene	9 – 18 Aug	45	1004		
H1	Isaac	21 Aug – 1 Sep	80	965	34	\$2.35B
TS	Joyce	22 – 24 Aug	40	1006		
H2	Kirk	28 Aug – 2 Sep	105	970		
H1	Leslie	30 Aug – 11 Sep	80	968		
H3	Michael	3 – 11 Sept	115	964		
H1	Nadine	10 Sept – 3 Oct	90	978		
TS	Oscar	3 – 5 Oct	50	994		
TS	Patty	11 – 13 Oct	45	1005		
H1	Rafael	12 – 17 Oct	90	969	1	
H3	Sandy	22 – 29 Oct	115	940	147	\$50B
TS	Tony	22 – 25 Oct	50	1000		

**RESULTS FOR THE
HURRICANE SEASON 2012
FROM REAL TIME
FORECASTS**

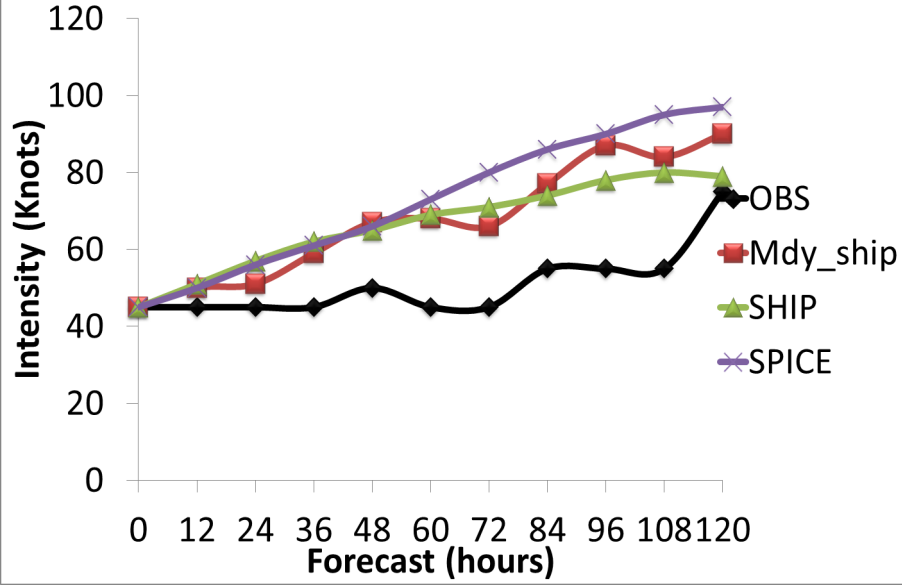
Debby.04I.2012062400



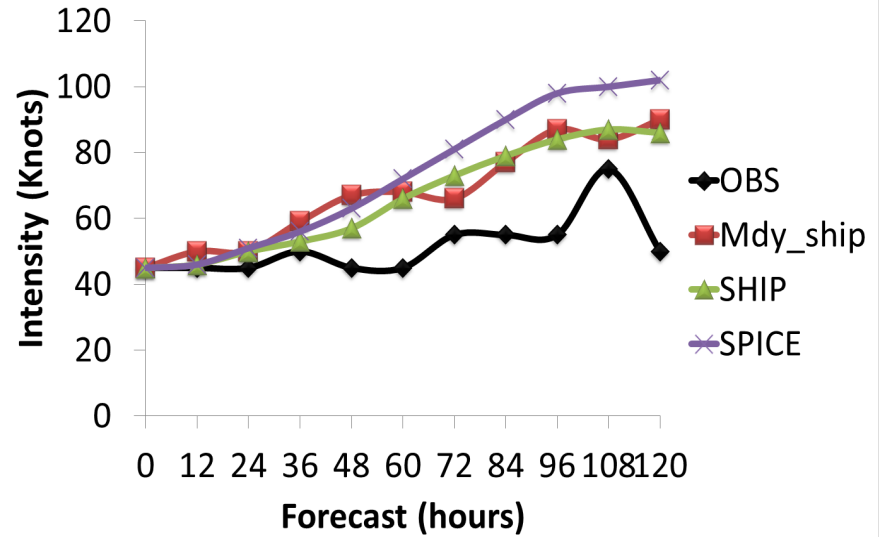
DEBBY.04I.2012062412



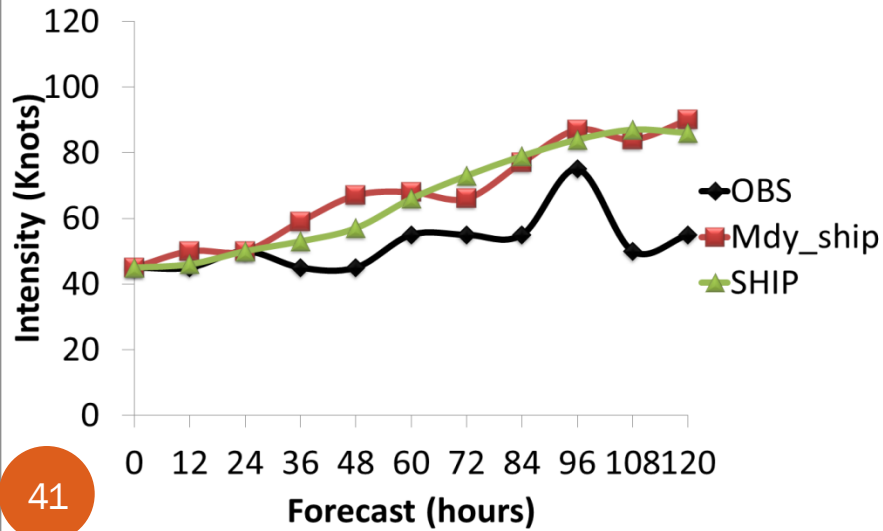
Ernesto.05l.2012080300



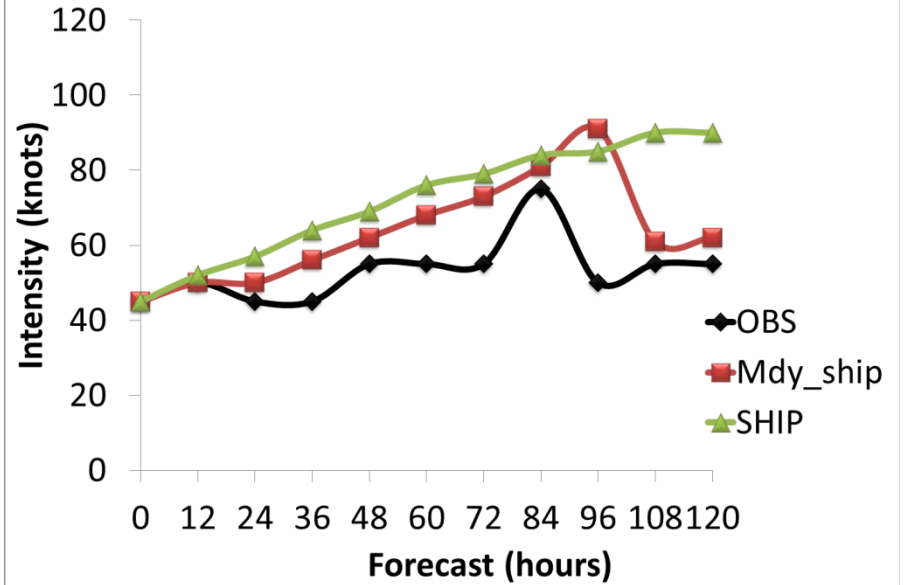
Ernesto.05l.2012080312



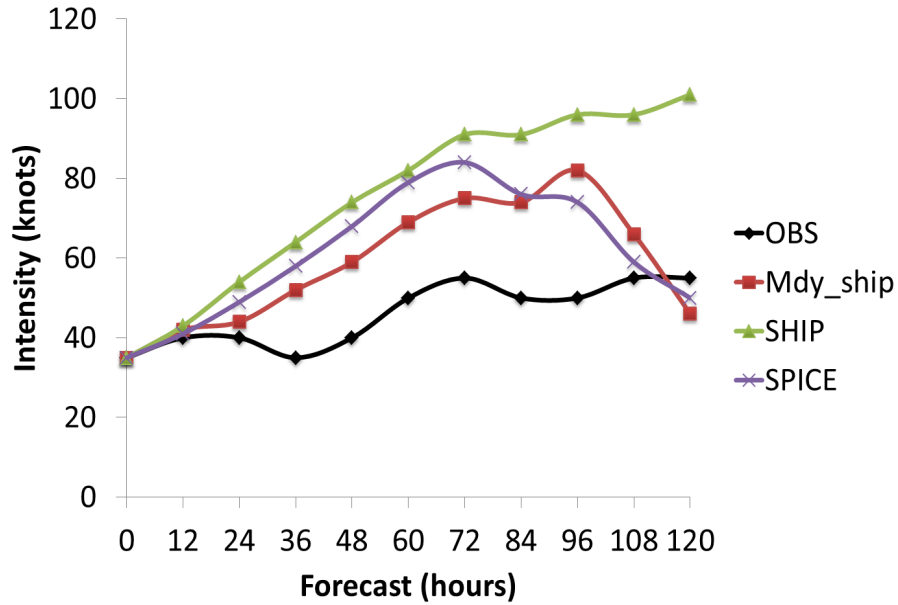
Ernesto.05l.2012080400



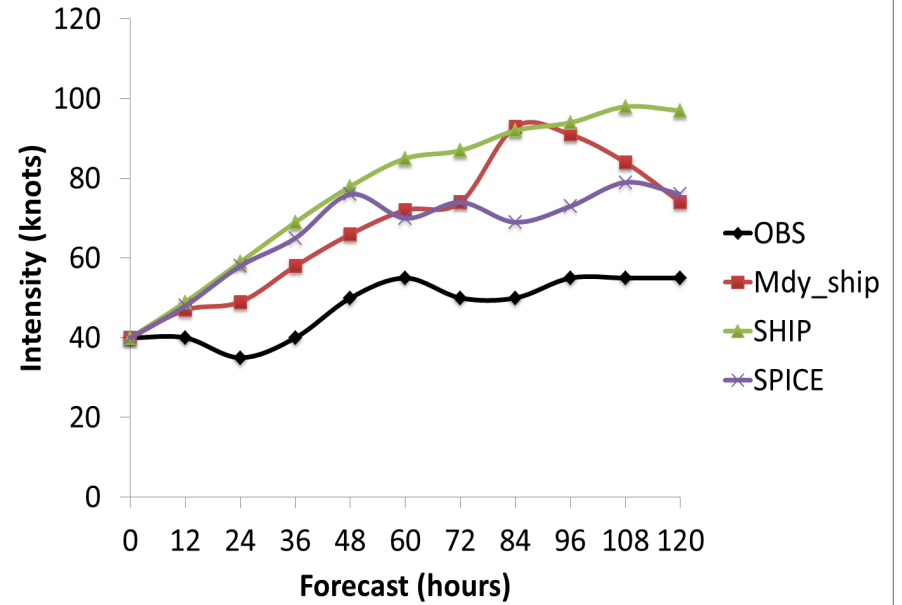
Ernesto.05l.2012080412



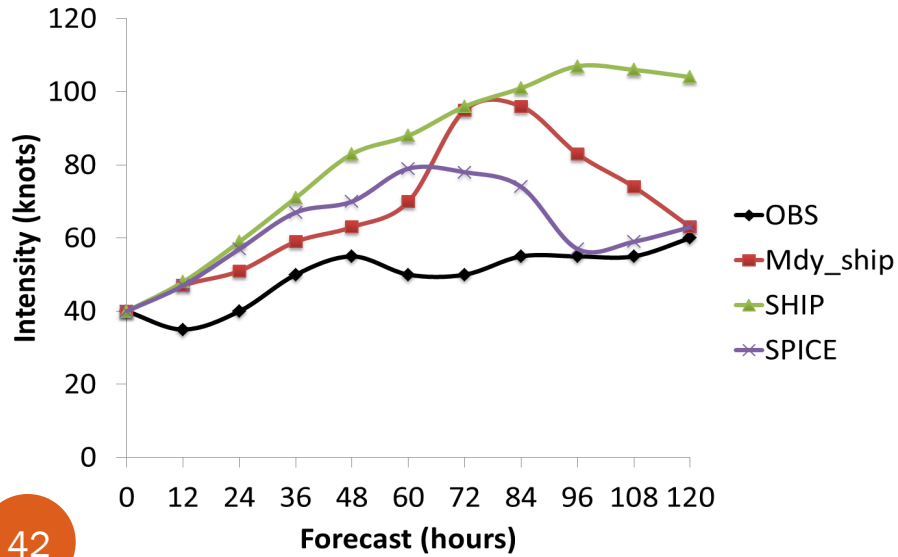
Isaac.09l.2012082200



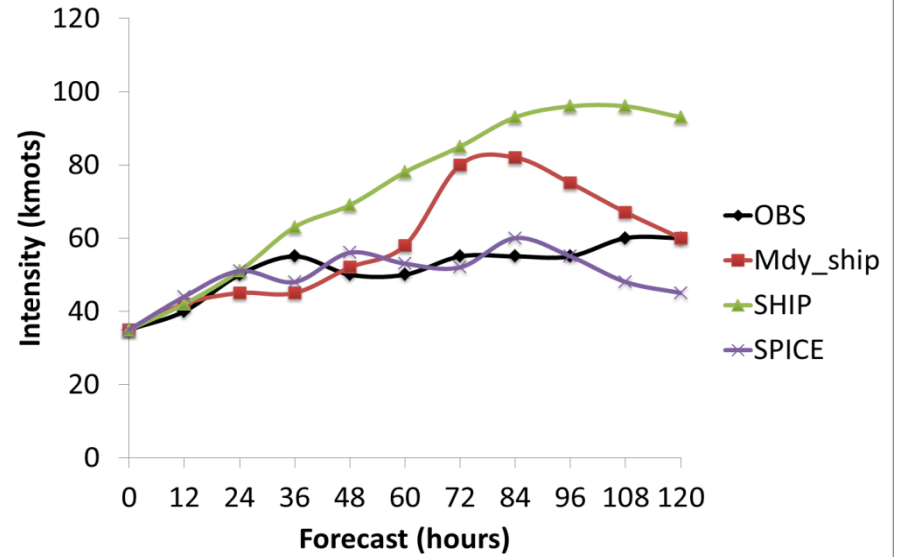
isaac.09l.2012082212



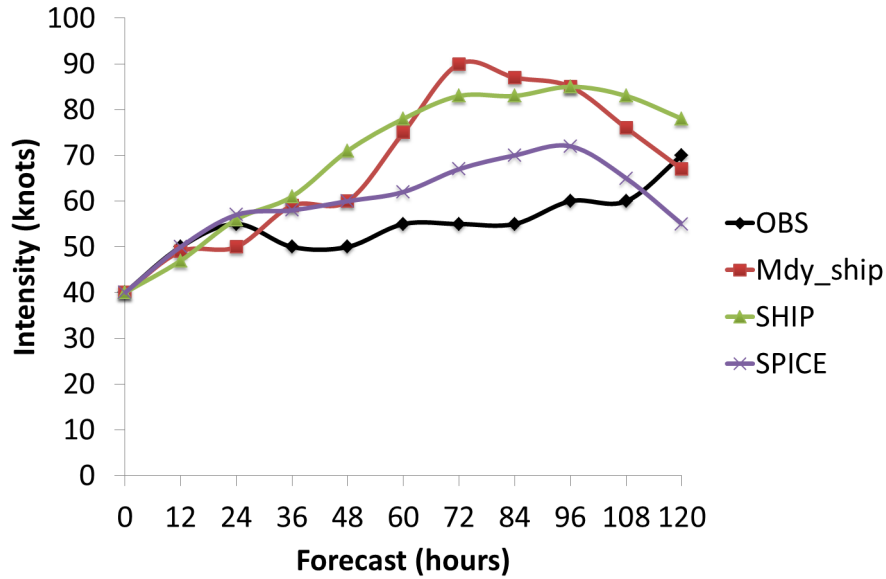
Isaac.09.2012082300



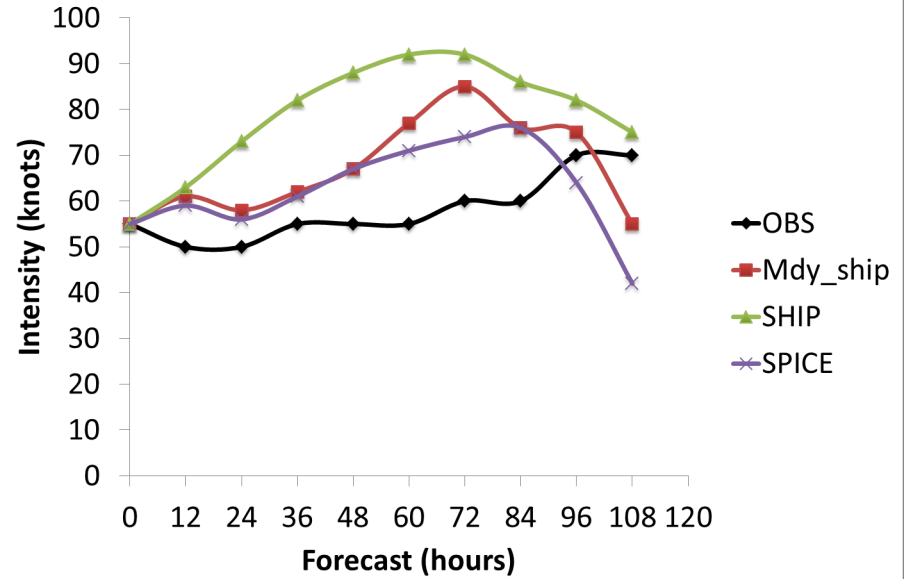
Isaac.09l.2012082312



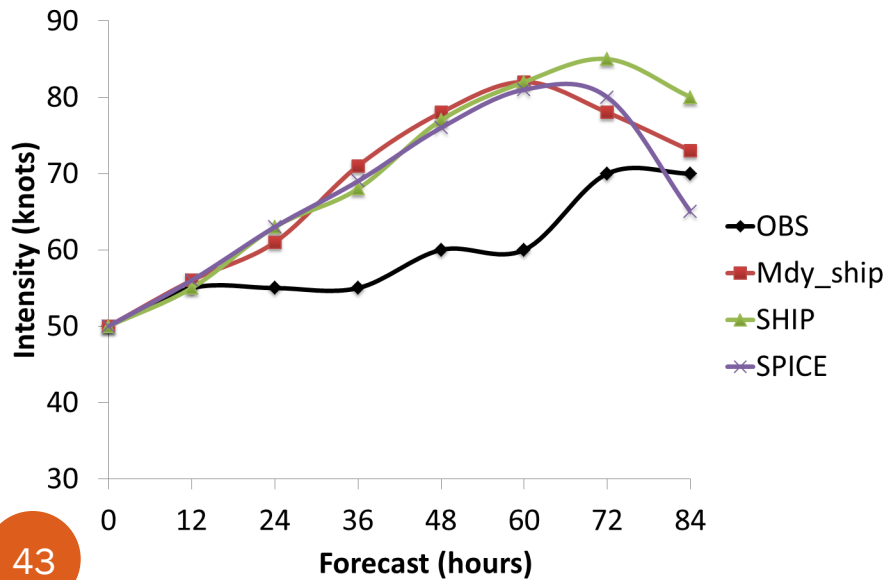
Isaac.09I.2012082400



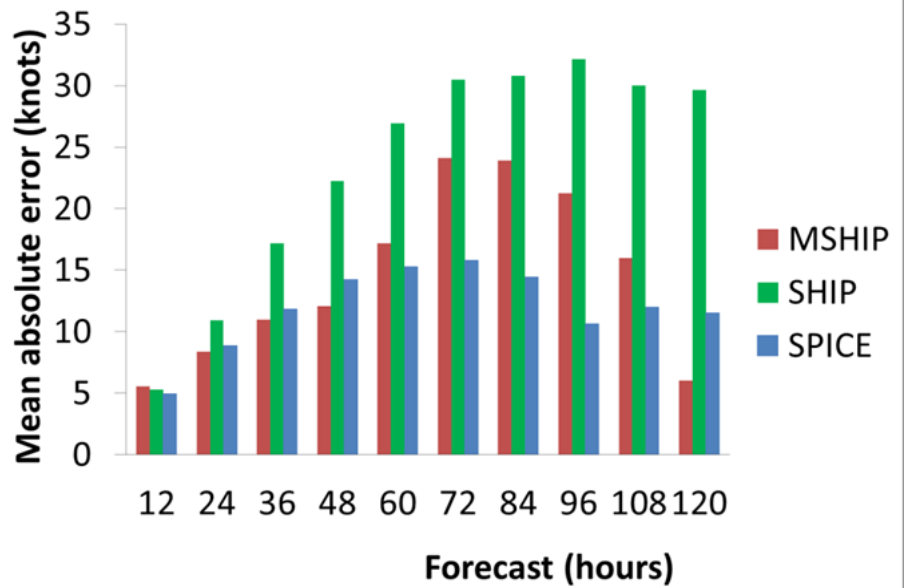
Isaac.09I.2012082500



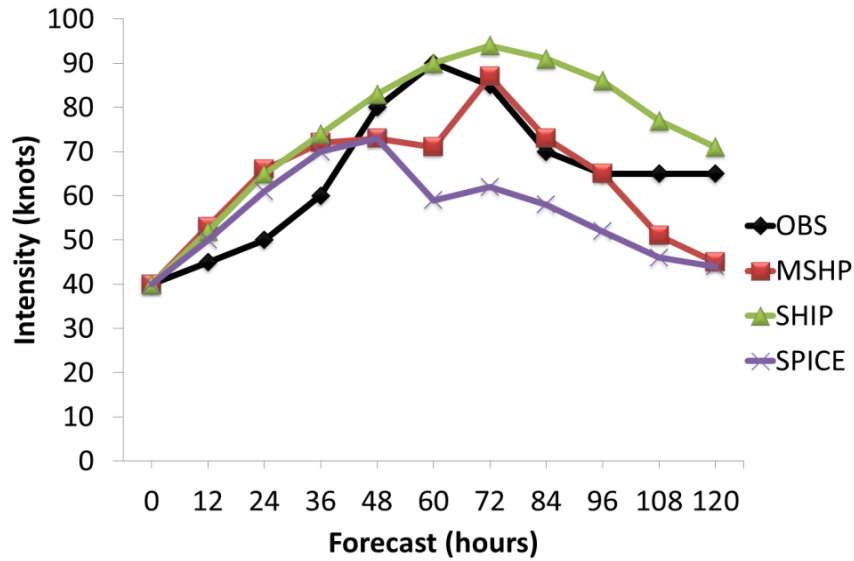
Isaac.09I.2012082600



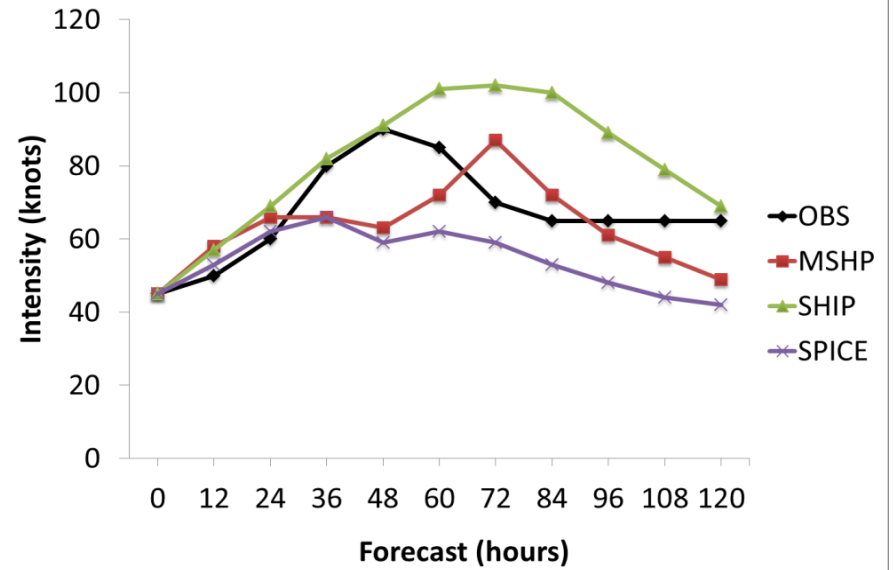
ISAAC FORECAST



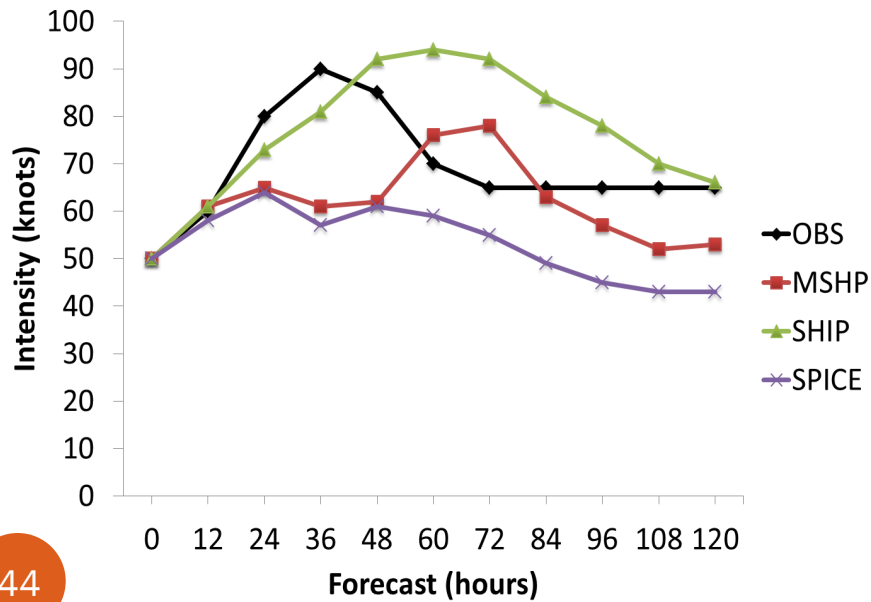
SANDY 2012102300



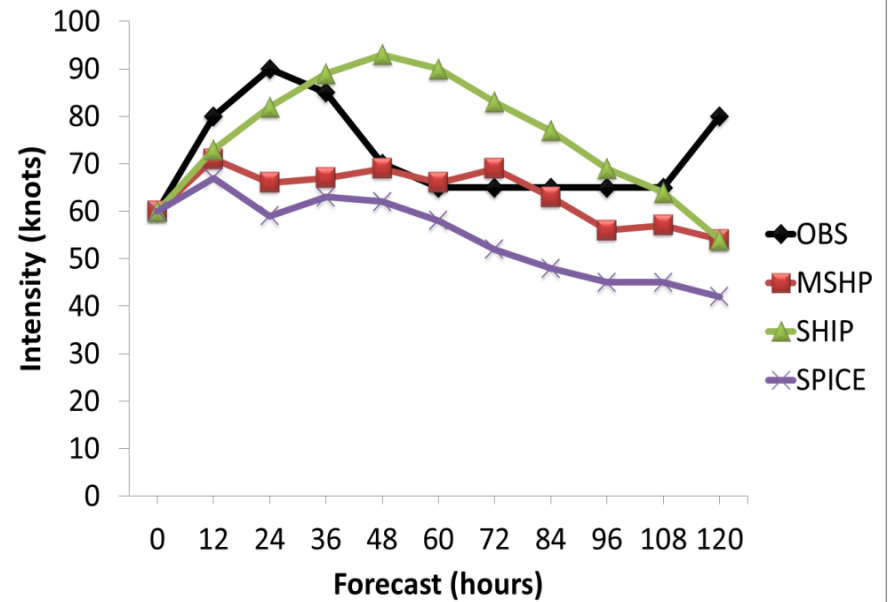
SANDY 2012102312



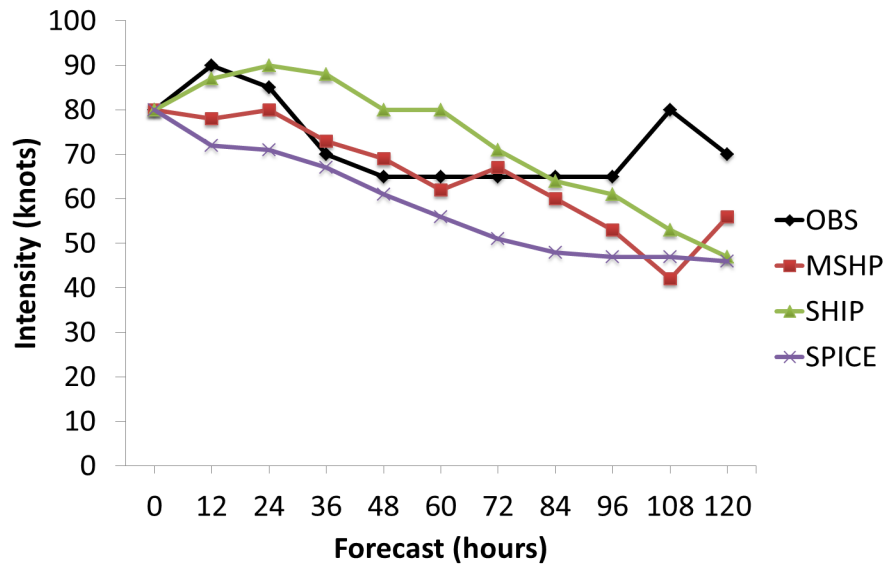
SANDY 2012102400



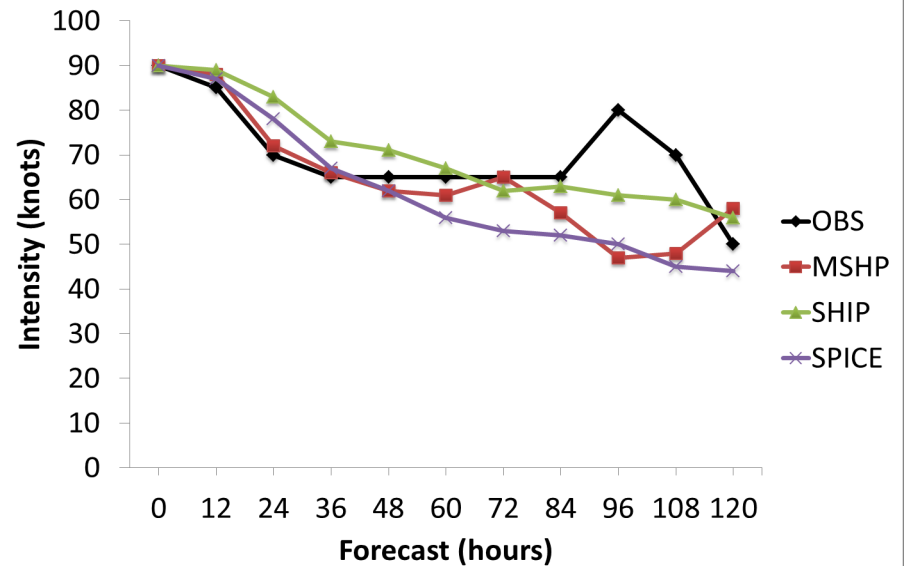
SANDY 2012102412



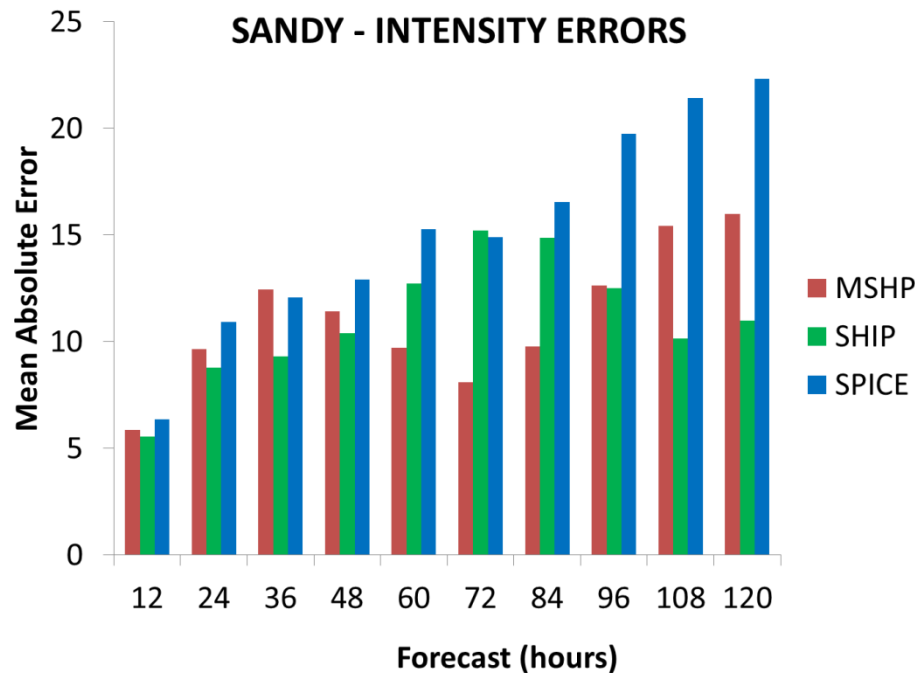
SANDY 2012102500



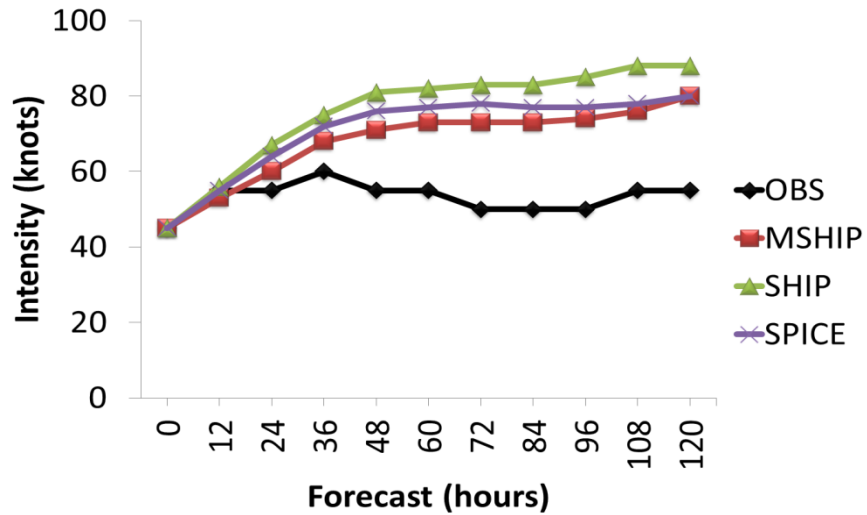
SANDY 2012102512



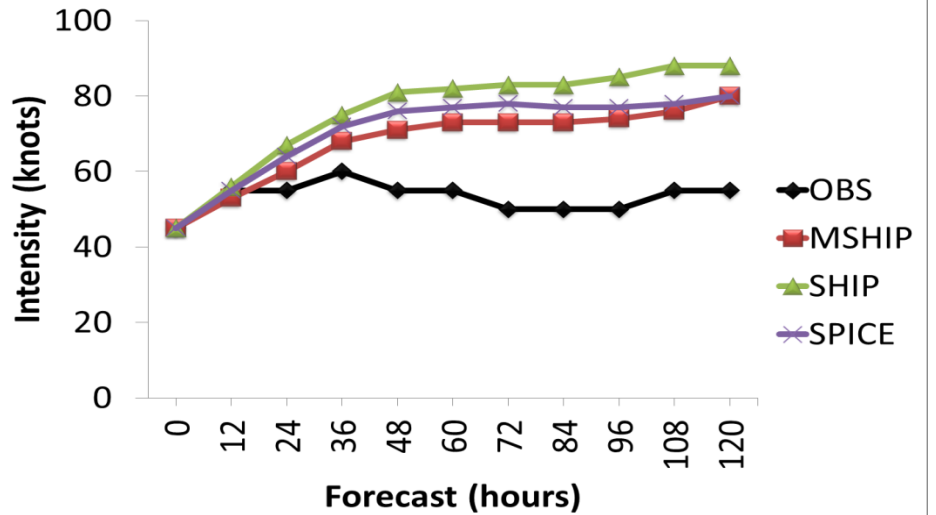
SANDY - INTENSITY ERRORS



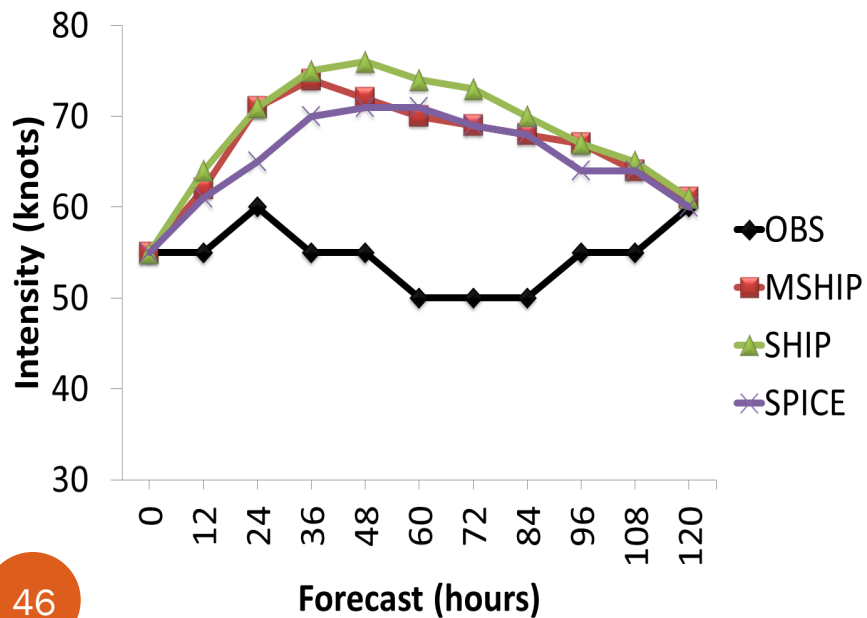
LESLIE 2012083100



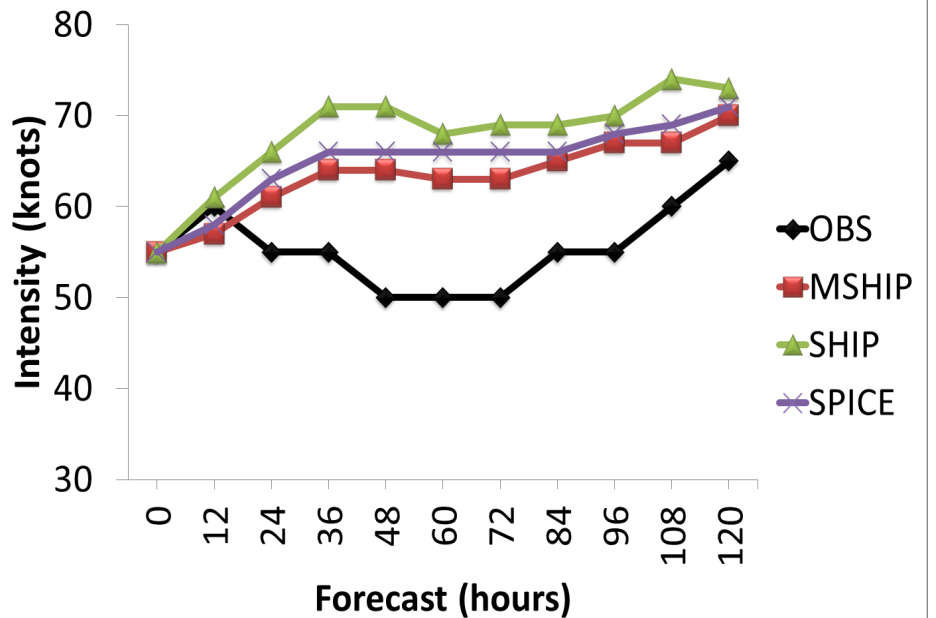
LESLIE 2012083100



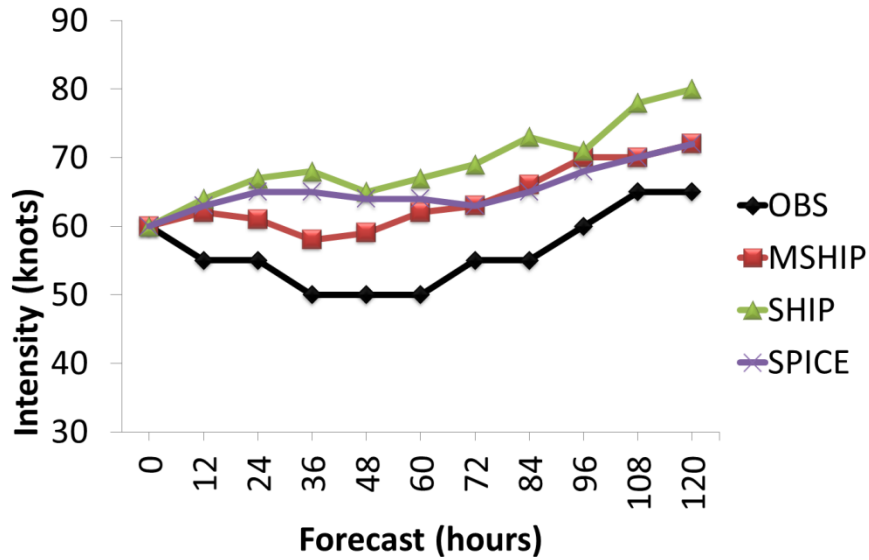
LESLIE 2012083112



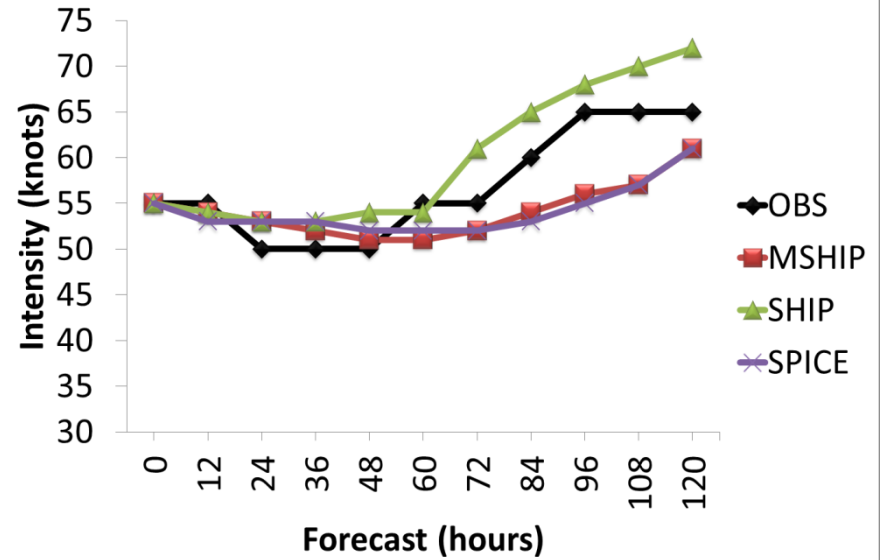
LESLIE 2012090100



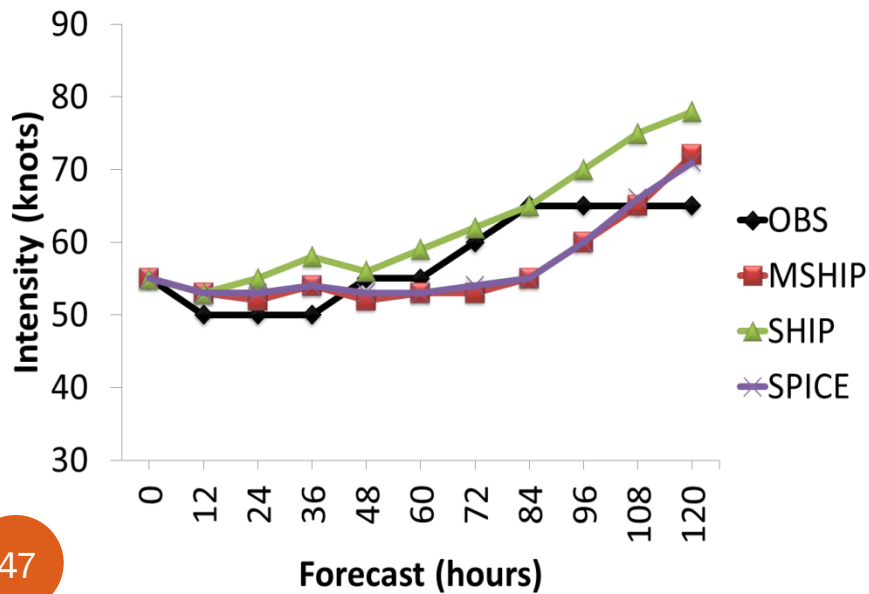
LESLIE 2012090112



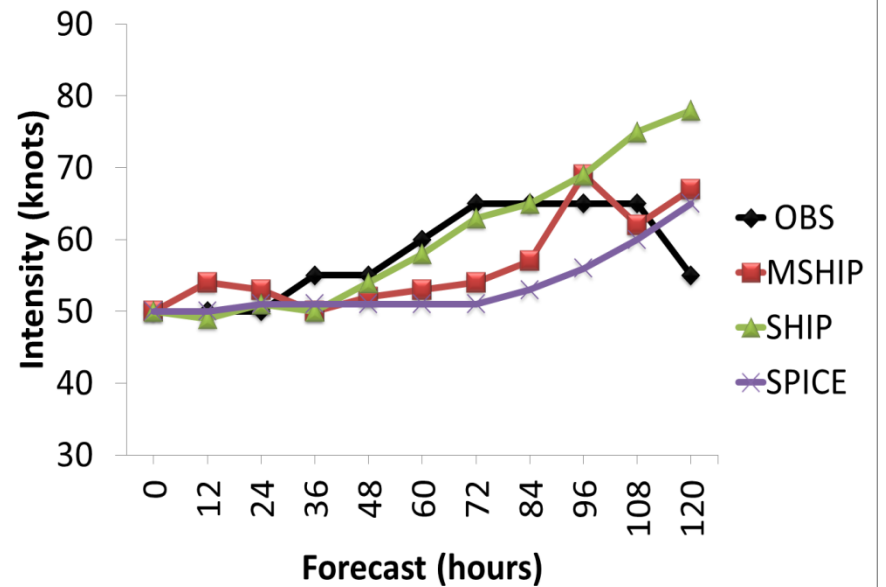
LESLIE 2012090200



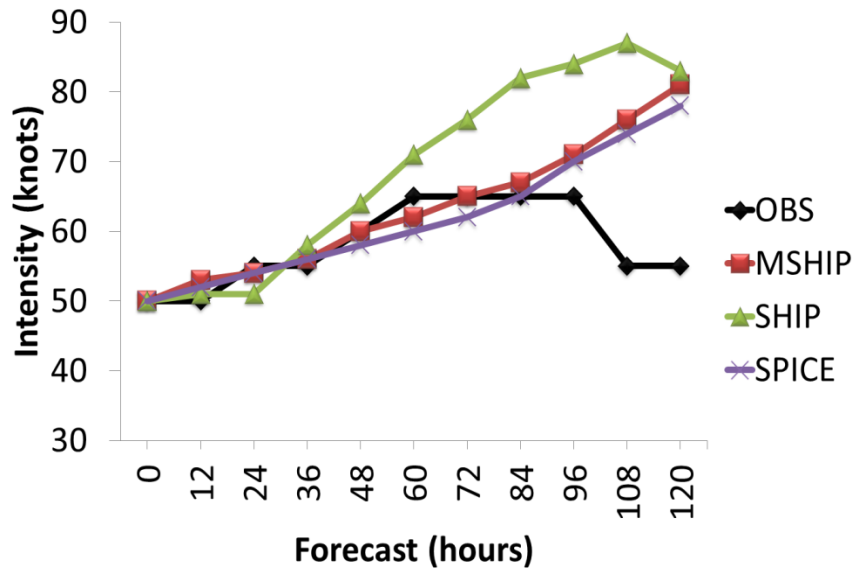
LESLIE 2012090212



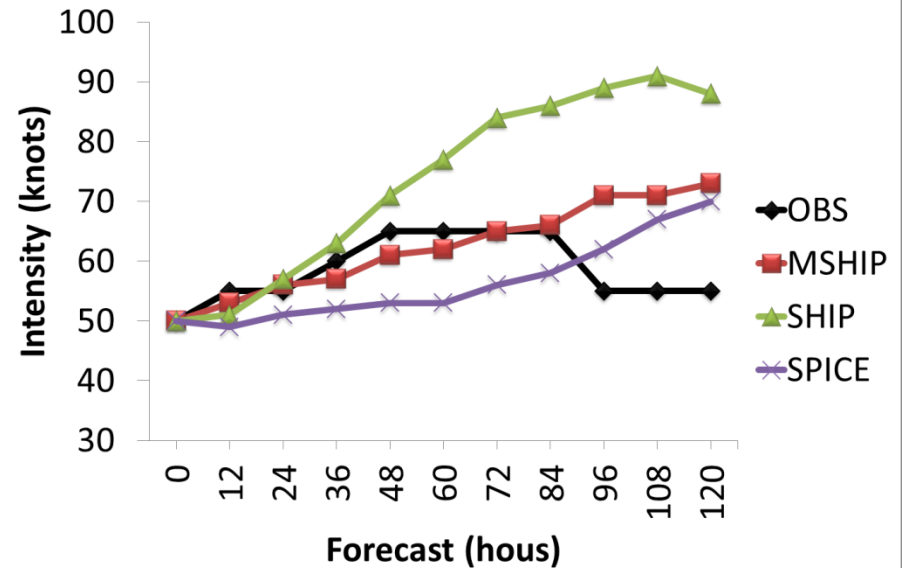
LESLIE 2012090300



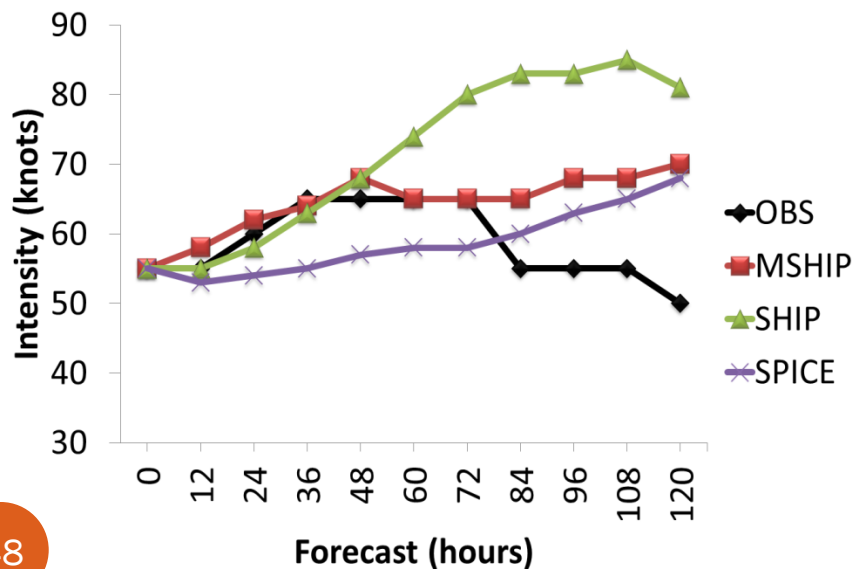
LESLIE 2012090312



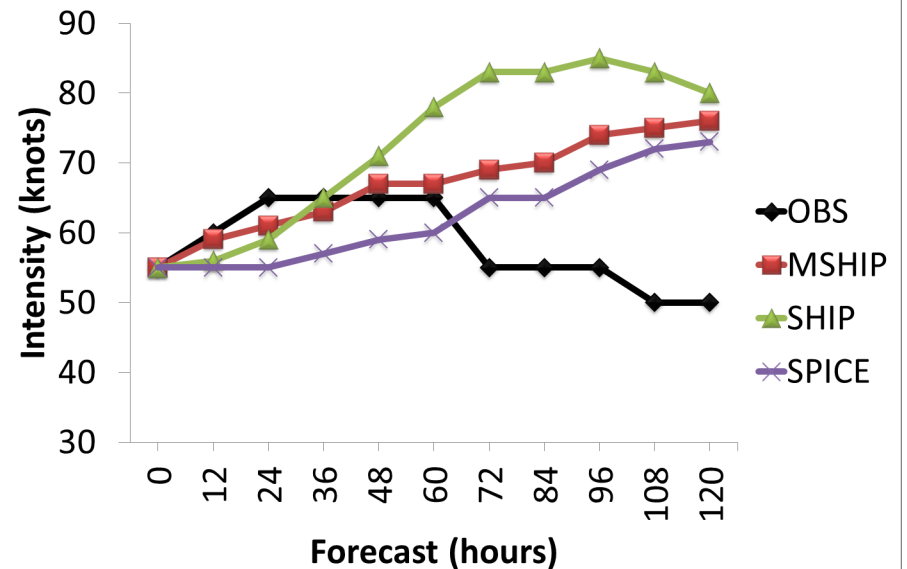
LESLIE 2012090400



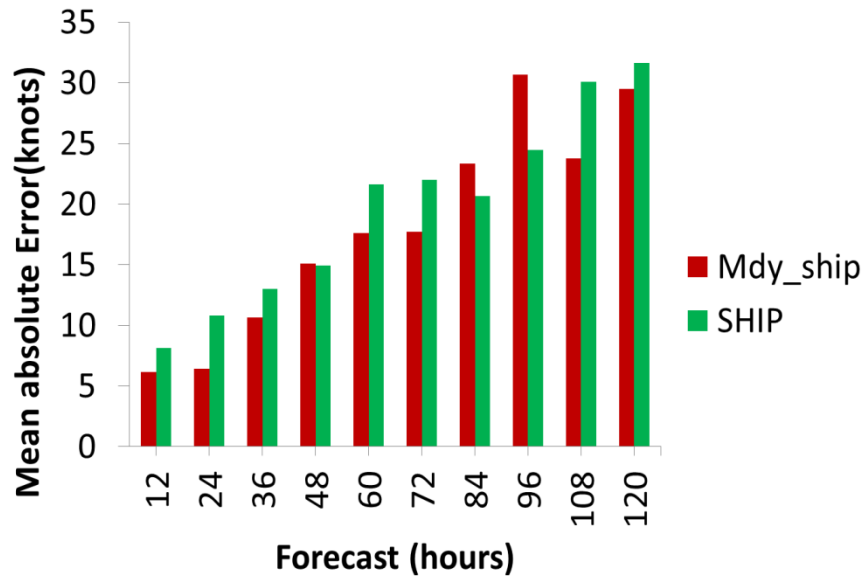
LESLIE 2012090412



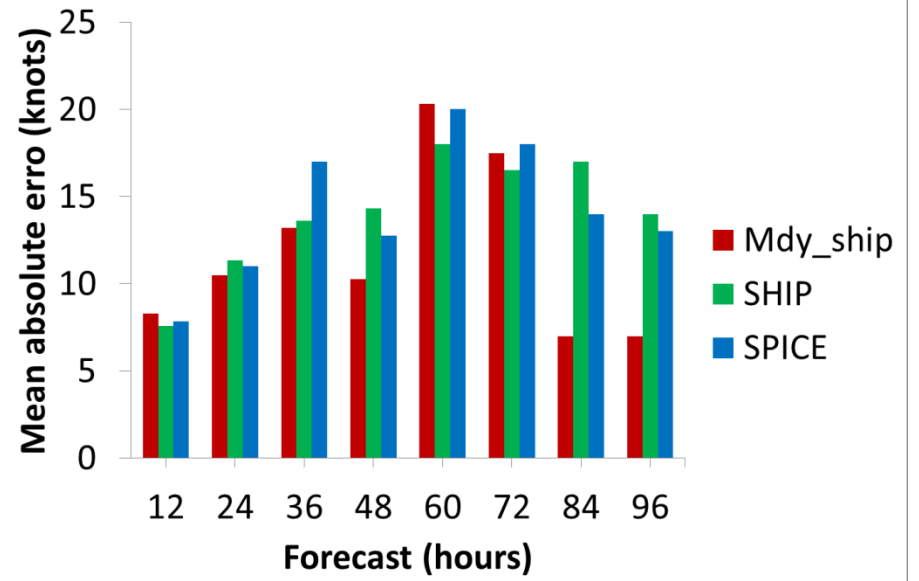
LESLIE 2012090500



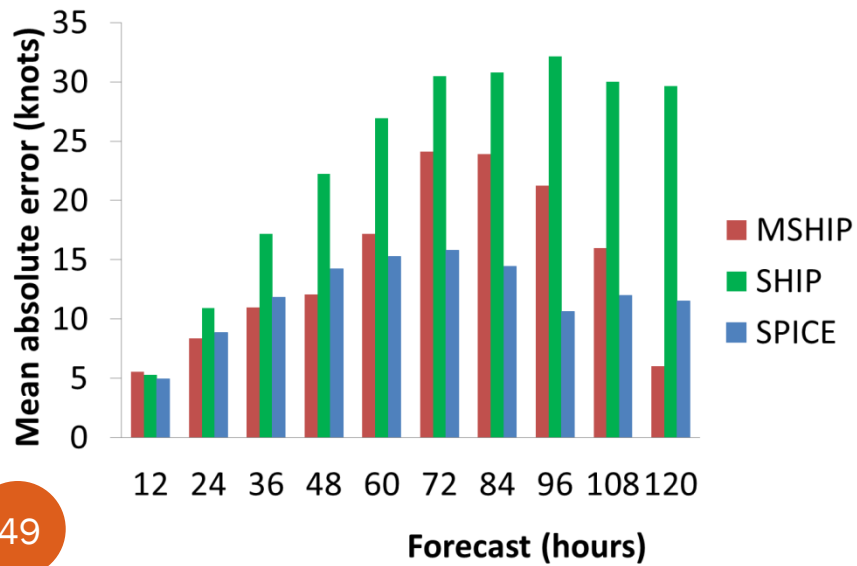
ERNESTO FORECAST



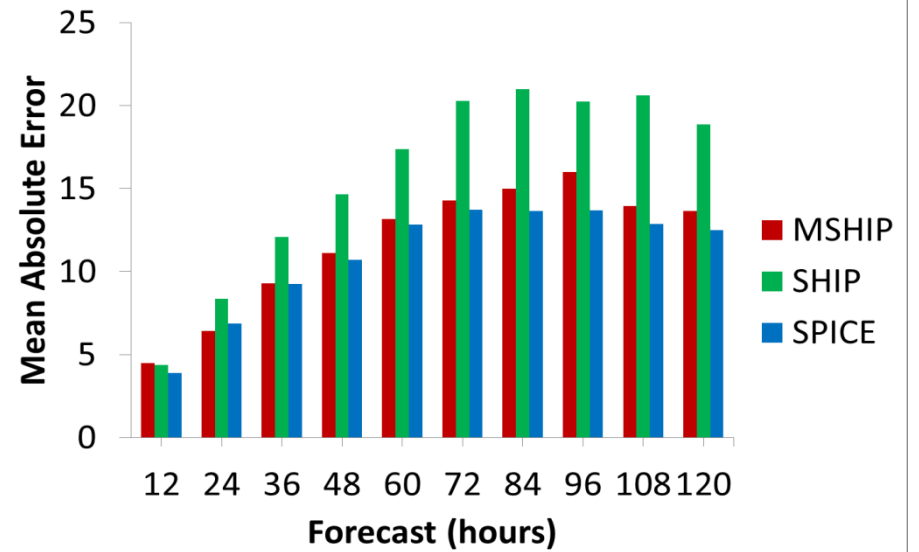
GORDON FORECAST

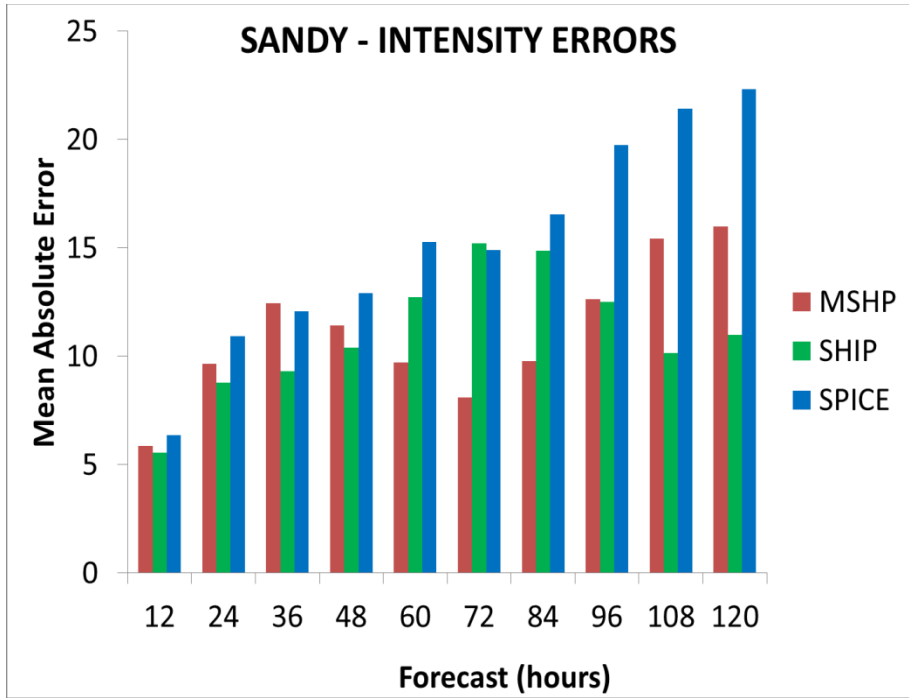
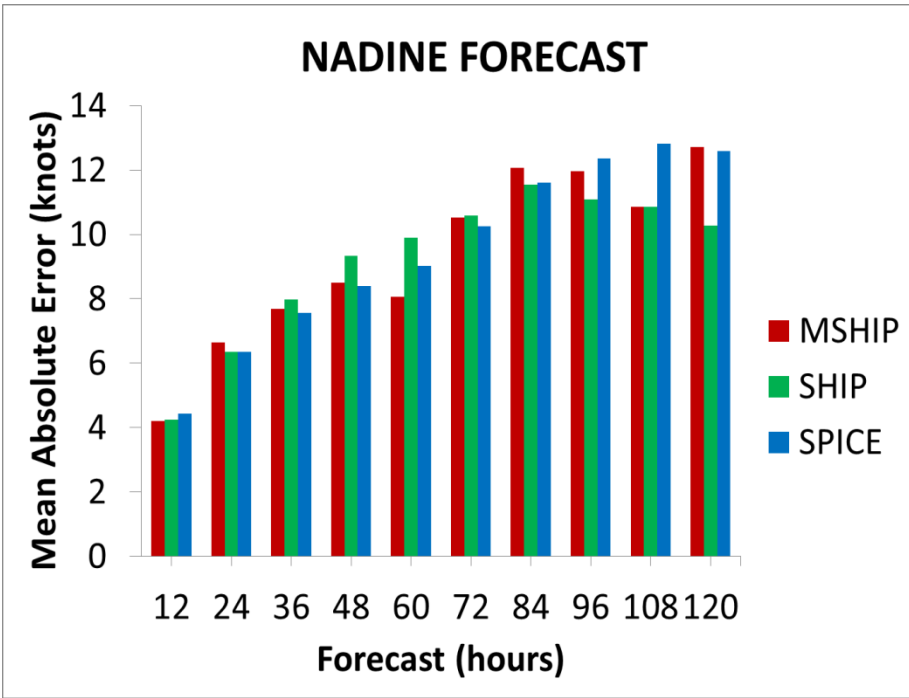


ISAAC FORECAST

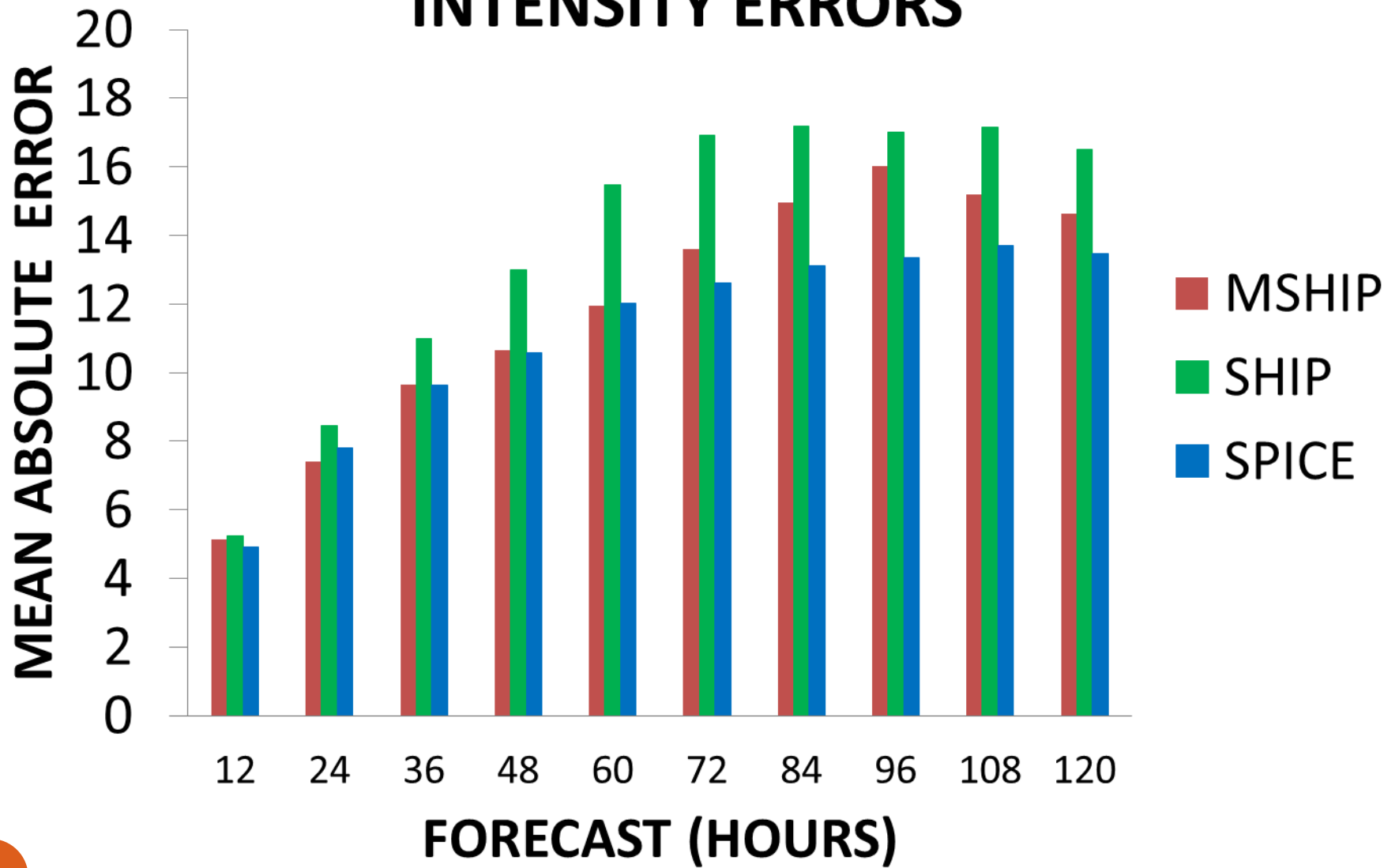


LESLIE STORM FORECAST



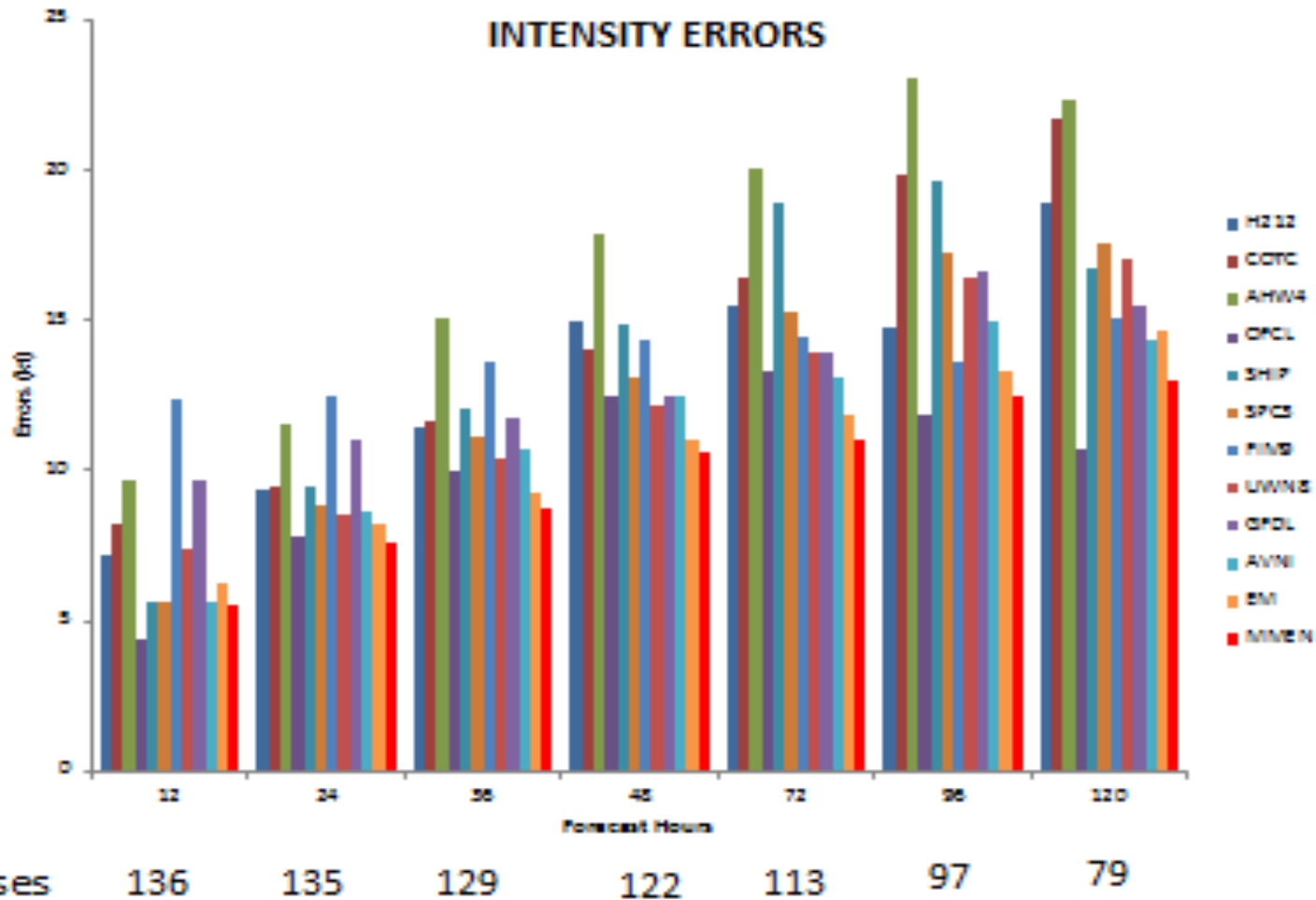


2012 All NAMED STORMS INTENSITY ERRORS



Multimodel Superensemble Results

2012 all storms



CONCLUSIONS

- **FSU EXTENDED SHIPS/SPICE ALGORITHM FOR HURRICANE INTENSITY FORECAST IMPROVEMENTS IS ALMOST READY FOR OPERATIONS.**
- **THE FSU DIAGNOSTIC VARIABLES BASED ON DIABATIC PV, ANGULAR MOMENTUM TRANSPORTS INTO HURRICANE CORE, ENERGY PROVIDED BY DIVERGENT WINDS AND THE SHEAR TO CURVATURE KINEMATICS PROVIDE GREAT STRENGTHS TO THE CURRENT SHIPS AND THE SPICE FORECAST PARAMETERS.**
- **THE FORECASTS, FOR THE NAMED STORMS OF 2012, FROM THE FSU MODIFIED SHIPS DO CONSISTENTLY PERFORM BETTER IN REDUCING THE INTENSITY ERRORS COMPARED TO THE SHIPS. FOR THE FIRST 72 HOURS THE SKILL OF THE MODIFIED SHIPS ARE COMPARABLE OR SLIGHTLY BETTER THAN THOSE OF SPICE. THEREAFTER SPICE HOLDS A SLIGHT EDGE IN ITS PERFORMANCE FOR THE REDUCTION OF INTENSITY ERRORS.**

➤ THE FOLLOWING COMMENT IS WORTH MENTIONING HERE : THE FSU MULTIMODEL SUPERENSEMBLE, THAT INCLUDES LARGELY A SUITE OF MESOSCALE MODELS PROVIDED THE LEAST ERRORS FOR THE HURRICANE INTENSITY FORECASTS , OUT TO 120 HOURS. THAT SUITE OF MODEL DOES INCLUDE THE SPICE AND SHIPS. THAT SUGGESTS THAT THE INCLUSION OF A LARGE SUITE OF MODELS WITHIN THE FRAMEWORK OF THE MULTIMODEL SUPERENSEMBLE CAN PROVIDE MUCH HIGHER SKILLS COMPARED TO SHIPS AND SPICE.

➤ FURTHER WORK IS STILL NEEDED TO BEST REPRESENT , USING SINGLE PARAMETERS, THE FOUR FSU DIAGNOSTIC VARIABLES. THIS IS OUR PRESENT ONGOING RESEARCH.

A satellite image of Earth showing a large hurricane over the Atlantic Ocean. The hurricane has a distinct eye and spiral cloud bands. The surrounding ocean is dark blue, and the landmasses of North and South America are visible in shades of green and brown. The text "THANK YOU" is overlaid in a large, red, serif font across the center of the image.

THANK YOU

Question ??